

Chapter 7. Nonlinear Response Theory

- 7.1 Kubo's form for the nonlinear response
- 7.2 Kawasaki Distribution Function
- 7.3 The Transient Time Correlation Formalism
- 7.4 Trajectory Mappings
- 7.5 Numerical Results for the Transient Time Correlation Functions
- 7.6 The Differential Response Function
- 7.7 Numerical results for the Kawasaki representation
- 7.8 The van Kampen Objection to Linear Response theory

7.1 Kubo's form for the nonlinear response

In Chapter 6 we saw that nonequilibrium molecular dynamics leads inevitably to questions regarding the nonlinear response of systems. In this chapter we will begin a discussion of this subject.

It is not widely known that in Kubo's original 1957 paper (Kubo, 1957), he not only presented results for adiabatic linear response theory, but that he also included a formal treatment of the adiabatic nonlinear response. The reason why this fact is not widely known is that, like many treatments of nonlinear response theory that followed, his formal results were exceedingly difficult to translate into a useful, experimentally verifiable forms. This difficulty can be traced to three sources. Firstly, his results are not easily transformable into explicit representations that involve the evaluation of time correlation functions of explicit phase variables. Secondly, if one wants to study nonequilibrium steady states, the treatment of thermostats is mandatory. His theory did not include such effects. Thirdly, his treatment gave a power series representation of the nonlinear response. We now believe that for most transport processes, such expansions do not exist.

We will now give a presentation of Kubo's perturbation expansion for the nonequilibrium distribution function, $f(t)$. Consider an N -particle system evolving under the following dynamics,

$$\begin{aligned}\dot{\mathbf{q}}_i &= \frac{\mathbf{p}_i}{m} + \mathbf{C}_i(\mathbf{\Gamma}) F_e \\ \dot{\mathbf{p}}_i &= \mathbf{F}_i - \mathbf{D}_i(\mathbf{\Gamma}) F_e\end{aligned}\tag{7.1.1}$$

The terms $\mathbf{C}_i(\mathbf{\Gamma})$ and $\mathbf{D}_i(\mathbf{\Gamma})$ describe the coupling of the external field F_e to the system. In this discussion we will limit ourselves to the case where the field is *switched on* at time zero, and thereafter remains at the same steady value. The f -Liouvillean is given by

$$iL = \mathbf{\Gamma} \cdot \frac{\partial}{\partial \mathbf{\Gamma}} + \frac{\partial}{\partial \mathbf{\Gamma}} \cdot \mathbf{\Gamma} = iL_0 + i\Delta L\tag{7.1.2}$$

where iL_0 is the equilibrium Liouvillean and $i\Delta L$ is the field dependent perturbation which is a linear function of F_e . The Liouville equation is,

$$\frac{\partial f(t)}{\partial t} = -iL f(t)\tag{7.1.3}$$

To go beyond the linear response treated in §5.1, Kubo assumed that $f(t)$ could be expanded as a

power series in the external field, F_e ,

$$f(t) = f_0 + f_1(t) + f_2(t) + f_3(t) + f_4(t) + \dots \quad (7.1.4)$$

where, $f_i(t)$ is i^{th} order in the external field F_e . The assumption that $f(t)$ can be expanded in a power series about $F_e = 0$ may seem innocent, but it is not. This assumption rules out any functional form containing a term of the form, F_e^α , where α is not an integer. Substituting (7.1.4) for $f(t)$, and the expression for iL , into the Liouville equation (7.1.3), and equating terms of the same order in F_e , we find an infinite sequence of partial differential equations to solve,

$$\frac{\partial f_i(t)}{\partial t} + iL_0 f_i(t) = -i\Delta L f_{i-1}(t) \quad (7.1.5)$$

where $i \geq 1$. The solution to this series of equations can be written as,

$$f_i(t) = - \int_0^t ds \exp(-iL_0(t-s)) i\Delta L f_{i-1}(s) \quad (7.1.6)$$

To prove that this is correct, one differentiates both sides of the equation to obtain (7.1.5). Recursively substituting (7.1.6), into equation (7.1.4), we obtain a power series representation of the distribution function

$$f(t) = f(0) + \sum_{i=1}^{\infty} (-1)^i \int_0^t ds_i \int_0^{s_{i-1}} ds_{i-1} \dots \int_0^{s_2} ds_2 e^{-iL_0(t-s)} \Delta L \dots e^{-iL_0(s_2-s_1)} \Delta L f(0) \quad (7.1.7)$$

Although this result is formally exact, there are a number of difficulties with this approach. The expression for $f(t)$ is a sum of convolutions of operators. In general the operator $i\Delta L$ does not commute with the propagator, $\exp(-iL_0 t)$, and no further simplifications of the general result are possible. Further, as we have seen in Chapter 6, there is a strong likelihood that fluxes associated with conserved quantities are non-analytic functions of the thermodynamic force, F_e . This would mean that the average response of the shear stress, for example, cannot be expanded as a Taylor series about $F_e (= \gamma) = 0$. In Chapter 6 we saw evidence that the shear stress is of the form, $\langle P_{xy} \rangle = -\gamma (\eta_0 + \eta_1 \gamma^{1/2})$ (see §6.3). If this is true then $f_2(t) (\equiv 1/2 \gamma^2 \partial^2 f(\gamma) / \partial \gamma^2 |_{\gamma=0})$ must be infinite.

7.2 Kawasaki Distribution Function

An alternative approach to nonlinear response theory was pioneered by Yamada and Kawasaki (1967). Rather than developing power series expansions about $F_e=0$, they derived a closed expression for the perturbed distribution function. The power of their method was demonstrated in a series of papers in which Kawasaki first predicted the non-analyticity of the shear viscosity with respect to strain rate (Kawasaki and Gunton, 1973, and Yamada and Kawasaki, 1975). This work predates the first observation of these effects in computer simulations. The simplest application of the Kawasaki method is to consider the adiabatic response of a canonical ensemble of N-particle systems to a steady applied field F_e .

The Liouville equation for this system is

$$\frac{\partial f}{\partial t} = -iL f \quad (7.2.1)$$

The Liouvillean appearing in this equation is the field dependent Liouvillean defined by the equations of motion, (7.1.1). Equation (7.2.1) has the formal solution,

$$f(t) = \exp[-iL t] f(0). \quad (7.2.2)$$

For simplicity we take the initial distribution function $f(0)$, to be canonical, so that $f(t)$ becomes

$$f(t) = e^{-iL t} \frac{e^{-\beta H_0}}{\int d\Gamma e^{-\beta H_0}} \quad (7.2.3)$$

The **adiabatic** distribution function propagator is the Hermitian conjugate of the phase variable propagator, so in this case $\exp(-iL t)$ is the negative-time phase variable propagator, $(\exp(iL(-t)))$. It operates on the phase variable in the numerator, moving time backwards in the presence of the applied field. This implies that

$$f(t) = \frac{e^{-\beta H_0(-t)}}{\int d\Gamma e^{-\beta H_0}} \quad (7.2.4)$$

Formally the f-propagator leaves the denominator invariant since it is not a phase variable. The phase dependence of the denominator has been integrated out. However since the distribution function must be normalised, we can obviously also write,

$$f(t) = \frac{e^{-\beta H_0(-t)}}{\int d\Gamma e^{-\beta H_0(-t)}} \quad (7.2.5)$$

This equation is an explicitly normalised version of (7.2.4) and we will have more to say concerning the relations between the so-called *bare* Kawasaki form, (7.2.4), and the renormalized Kawasaki form, (7.2.5), for the distribution function in §7.7. In Kawasaki's original papers he referred only to the *bare* Kawasaki form, (7.2.4).

Using the equations of motion (7.1.1) one can write the time derivative of H_0 as the product of a phase variable $J(\Gamma)$ and the magnitude of the perturbing external field, F_e .

$$\dot{H}_0^{\text{ad}} = -J(\Gamma) F_e \quad (7.2.6)$$

For the specific case of planar Couette flow, we saw in §6.2 that dH_0/dt^{ad} is the product of the strain rate, the shear stress and the system volume, $-\gamma P_{xy}V$ and thus in the absence of a thermostat we can write,

$$H_0(-t) = H_0(0) - \int_0^t ds \dot{H}_0(-s) = H_0(0) + \gamma V \int_0^t ds P_{xy}(-s) \quad (7.2.7)$$

The *bare* form for the perturbed distribution function at time t is then

$$f(t) = \exp \left[-\beta \gamma V \int_0^t ds P_{xy}(-s) \right] f(0) \quad (7.2.8)$$

It is important to remember that the generation of $P_{xy}(-s)$ from $P_{xy}(0)$ is controlled by the field-dependent equations of motion.

A major problem with this approach is that in an adiabatic system the applied field will cause the system to heat up. This process continues indefinitely and a steady state can never be reached. What is surprising is that when the effects of a thermostat are included, the formal expression for the N -particle distribution function remains unaltered, the only difference being that thermostatted, field-dependent dynamics must be used to generate $H_0(-t)$ from $H_0(0)$. This is the next result we shall derive.

Consider an isokinetic ensemble of N -particle systems subject to an applied field. We will assume field dependent, Gaussian isokinetic equations of motion, (5.3.1). The f -Liouvillean therefore contains an extra thermostating term. It is convenient to write the Liouville

equation in operator form

$$\frac{\partial f(t)}{\partial t} = -iL f(t) = -iL f(t) - f(t) \Lambda = -\frac{\partial}{\partial \Gamma} \cdot (\dot{\Gamma} f) \quad (7.2.9)$$

The operator iL is the f-Liouvillean, and iL is the p-Liouvillean. The term Λ ,

$$\Lambda = \frac{\partial}{\partial \Gamma} \cdot \dot{\Gamma} = -\frac{1}{f} \frac{df}{dt} = -\frac{d \ln f}{dt} \quad (7.2.10)$$

is the phase space compression factor (§3.3). The formal solution of the Liouville equation is given by

$$f(t) = \exp[-iL t] f(0) = \exp[-(iL + \Lambda)t] f(0), \quad (7.2.11)$$

In the thermostatted case the p-propagator is no longer the Hermitian conjugate of the f-propagator.

We will use the Dyson decomposition derived §3.6, to relate thermostatted p- and f-propagators. We assume that the both p-Liouvilleans have no explicit time dependence. We make a crucial observation, namely that the phase space compression factor Λ , is a phase variable rather than an operator. Taking the reference Liouvillean iL_0 , to be the adjoint of iL , we find

$$\exp[-iLt - \Lambda t] = \exp[-iLt] - \int_0^t ds \exp[-iLs - \Lambda s] \Lambda \exp[-iL(t-s)] \quad (7.2.12)$$

Repeated application of the Dyson decomposition to $\exp[-iLs - \Lambda s]$ on the right hand side gives

$$\begin{aligned} \exp[-iLt - \Lambda] &= \sum_{n=0}^{\infty} (-)^n \int_0^t ds_1 \dots \int_0^{s_{n-1}} ds_n \exp[-iLs_n] \Lambda \exp[-iL(s_{n-1} - s_n)] \Lambda \dots \exp[-iL(t-s_1)] \\ &= \sum_{n=0}^{\infty} (-)^n \int_0^t ds_1 \dots \int_0^{s_{n-1}} ds_n \Lambda(-s_n) \Lambda(-s_{n-1}) \dots \Lambda(-s_1) \exp[-iLt] \\ &= \exp\left[-\int_0^t ds \Lambda(-s)\right] \exp[-iLt] \end{aligned} \quad (7.2.13)$$

In deriving the second line of this equation we use the fact that for any phase variable B , $\exp[-iLs]B = B(-s)\exp[-iLs]$. Substituting (7.2.13) into (7.2.11) and choosing, $f(0) = f_T(0) = \delta(K - K_0) \exp(-\beta\Phi) / Z(\beta)$, we obtain

$$f(t) = \frac{\delta(K-K_0) \exp\left[-\int_0^t ds \Lambda(-s)\right] \exp(-\beta\Phi(-t))}{Z(\beta)} \quad (7.2.14)$$

If we change variables in the integral of the phase space compression factor and calculate $\Phi(-t)$ from its value at time zero we obtain,

$$f(t) = \frac{\delta(K-K_0) \exp(-\beta\Phi(0)) \exp\left[\int_0^{-t} ds \Lambda(s) - \beta\dot{\Phi}(s)\right]}{Z(\beta)} \quad (7.2.15)$$

We know that for the isokinetic distribution, $\beta = 3N/2K$ (see §5.2). Since under the isokinetic equations of motion, K , is a constant of the motion, we can prove from (5.3.1), that,

$$\Lambda - \beta d\Phi/dt = \beta J F_e. \quad (7.2.16)$$

If AIF is satisfied the dissipative flux, J , is defined by equation (7.2.6). Substituting (7.2.20) into (7.2.19) we find that the *bare* form of the thermostatted Kawasaki distribution function can be written as,

$$\begin{aligned} f_T(t) &= f_T(0) \exp\left[\beta \int_0^{-t} ds J(s) F_e\right] \\ &= f_T(0) \exp\left[-\beta \int_0^t ds J(-s) F_e\right] \end{aligned} \quad (7.2.17)$$

Formally this equation is identical to the adiabatic response (7.2.8). This is in spite of the fact that the thermostat changes the equations of motion. The adiabatic and thermostatted forms are identical because the changes caused by the thermostat to the dissipation (dH_0/dt), are **exactly** cancelled by the changes caused by the thermostat to the form of the Liouville equation. This observation was first made by Morriss and Evans (1985). Clearly one can renormalize the thermostatted form of the Kawasaki distribution function giving (7.2.18), as the renormalized form of the isokinetic Kawasaki distribution function, $f_{\text{Trn}}(t)$.

$$f_{\text{Trn}}(t) = \frac{\exp\left[-\beta \int_0^t ds J(-s) F_e\right] f_T(0)}{\left\langle \exp\left[-\beta \int_0^t ds J(-s) F_e\right] \right\rangle} \quad (7.2.18)$$

As we will see, the renormalized Kawasaki distribution function is very useful for deriving relations between steady state fluctuations and derivatives of steady state phase averages. However, it is not useful for computing nonequilibrium averages themselves. This is because it involves averaging exponentials of integrals which are extensive. We will now turn to an alternative approach to this problem.

7.3 The Transient Time Correlation Function Formalism

The Transient Time Correlation Function formalism (TTCF), provides perhaps the simplest nonlinear generalisation of the Green-Kubo relations. A number of authors independently derived the TTCF expression for adiabatic phase averages, (W.M. Visscher, 1974, Dufty and Lindenfeld, 1979 and Cohen, 1983). We will illustrate the derivation for isokinetic planar Couette flow. However the formalism is quite general and can easily be applied to other systems. The theory gives an exact relation between the nonlinear steady state response and the so-called transient time correlation functions. We will also describe the links between the TTCF approach and the Kawasaki methods outlined in §7.2. Finally, we will present some numerical results which were obtained as tests of the validity of the TTCF formalism.

Following Morriss and Evans, (1987), we will give our derivation using the Heisenberg, rather than the customary Schrödinger picture. The average of a phase variable, $B(\Gamma)$, at time, t , is,

$$\langle B(t) \rangle = \int d\Gamma B(\Gamma) f(t) = \int d\Gamma f(0) B(\Gamma; t) \quad (7.3.1)$$

where the second equality is a consequence of the Schrödinger-Heisenberg equivalence. For **time independent** external fields, differentiating the Heisenberg form with respect to time yields,

$$\frac{d\langle B(t) \rangle}{dt} = \int d\Gamma f(0) \Gamma \cdot \frac{\partial B(t)}{\partial \Gamma} \quad (7.3.2)$$

In deriving (7.3.2) we have used the fact that, $dB(t)/dt = iL \exp(iLt) B = \exp(iLt) iLB$. This relies upon the time independence of the Liouvillean, L . The corresponding equation for the time dependent case, is not true. Integrating (7.3.2) by parts we see that,

$$\frac{d\langle B(t) \rangle}{dt} = - \int d\Gamma B(t) \frac{\partial}{\partial \Gamma} \cdot (\Gamma f(0)) \quad (7.3.3)$$

The boundary term vanishes because: the distribution function, $f(0)$, approaches zero when the magnitude of any component of any particle's momentum becomes infinite, and because the distribution function can be taken to be a periodic function of the particle coordinates. We are explicitly using the periodic boundary conditions used in computer simulations.

Integrating (7.3.3) with respect to time we see that the nonlinear nonequilibrium response can be written as,

$$\langle B(t) \rangle = \langle B(0) \rangle - \int_0^t ds \int d\Gamma B(s) \frac{\partial}{\partial \Gamma} \cdot \dot{\Gamma} f(0) \quad (7.3.4)$$

The dynamics implicit in $B(s)$, is of course driven by the full field-dependent, thermostatted equations of motion ((7.1.1) and (7.1.2)). For a system subject to the thermostatted shearing deformation, $d\Gamma/dt$ is given by the thermostatted SLLOD equations of motion, (6.3.22).

If the initial distribution is Gaussian isokinetic it is straightforward to show that, $(\partial/\partial \Gamma) \cdot (f(0) d\Gamma/dt) = \beta V P_{xy} f(0)$. If the initial ensemble is canonical then, to first order in the number of particles, $(\partial/\partial \Gamma) \cdot (f(0) d\Gamma/dt)$ is $\beta V P_{xy} f(0)$. To show this one writes, (following §5.3),

$$\langle B(t) \rangle_C = \langle B(0) \rangle_C - \beta \mathcal{W} \int_0^t ds \langle B(s) [P_{xy}(0) - P_{xy}^K(0) \frac{\Delta(K(0))}{\langle K \rangle_C}] \rangle_C \quad (7.3.5)$$

where $P_{xy}^K(0)$ is the kinetic part of the pressure tensor evaluated at time zero (compare this with the linear theory given in §5.3). Now we note that $\langle P_{xy}^K(0) \Delta(K(0))/\langle K \rangle_C \rangle_C = 0$. This means that equation (7.3.5) can be written as,

$$\langle B(t) \rangle_C = \langle B(0) \rangle_C - \beta \mathcal{W} \int_0^t ds \langle \Delta(B(s)) [P_{xy}(0) - P_{xy}^K(0) \frac{\Delta(K(0))}{\langle K \rangle_C}] \rangle_C \quad (7.3.6)$$

As in the linear response case (§5.3), we assume, without loss of generality, that B is extensive. The kinetic fluctuation term involves the average of three zero mean, extensive quantities and because of the factor $1/\langle K(0) \rangle$, gives only an order one contribution to the average. Thus for both the isokinetic and canonical ensembles, we can write,

$$\langle B(t) \rangle = \langle B(0) \rangle - \beta \gamma V \int_0^t ds \langle \Delta(B(s)) P_{xy}(0) \rangle \quad (7.3.7)$$

This expression relates the non-equilibrium value of a phase variable B at time t , to the integral of a transient time correlation function (the correlation between P_{xy} in the equilibrium starting state, $P_{xy}(0)$, and B at time s after the field is turned on). The time zero value of the transient correlation function is an equilibrium property of the system. For example, if $B = P_{xy}$, then the time zero value is $\langle P_{xy}^2(0) \rangle$. Under some, but by no means all circumstances, the values of

$B(s)$ and $P_{xy}(0)$ will become uncorrelated at long times. If this is the case the system is said to exhibit mixing. The transient correlation function will then approach $\langle B(t) \rangle \langle P_{xy}(0) \rangle$, which is zero because $\langle P_{xy}(0) \rangle = 0$.

The adiabatic systems treated by Visscher, Dufty, Lindenfeld and Cohen do not exhibit mixing because in the absence of a thermostat, $d\langle B(t) \rangle / dt$ does not, in general, go to zero at large times. Thus the integral of the associated transient correlation function does not converge. This presumably means that the initial fluctuations in adiabatic systems are remembered forever. Other systems which are not expected to exhibit mixing are turbulent systems or systems which execute quasi-periodic oscillations.

If $A\Gamma$ (§5.3) is satisfied, the result for the general case is,

$$\langle B(t) \rangle = \langle B(0) \rangle - \beta F_e \int_0^t ds \langle \Delta B(s) J(0) \rangle \quad (7.3.8)$$

We can use recursive substitution to derive the Kawasaki form for the nonlinear response from the transient time correlation formula, equation (7.3.8). The first step in the derivation of the Kawasaki representation is to rewrite the TTCF relation using iL to denote the phase variable Liouvillean, and $-iL$ to denote its nonhermitian adjoint, the f-Liouvillean. Thus $dB/dt \equiv iLB$ and $\partial f/\partial t \equiv -iL f$. Using this notation equation (7.3.8) can be written as,

$$\langle B(t) \rangle = \int d\Gamma B f(0) - \beta \gamma \mathcal{V} \int_0^t ds \int d\Gamma f(0) e^{iLs} B e^{-iLs} J \quad (7.3.9)$$

$$= \int d\Gamma B f(0) - \beta \gamma \mathcal{V} \int_0^t ds \int d\Gamma (e^{iLs} f(0)) B e^{-iLs} J \quad (7.3.10)$$

where we have unrolled the first p-propagator onto the distribution function. Equation (7.3.10) can be written more simply as,

$$\langle B(t) \rangle = \int d\Gamma B f(0) - \beta \gamma \mathcal{V} \int_0^t ds \int d\Gamma B(0) J(-s) f(s) \quad (7.3.11)$$

Since this equation is true for all phase variables B , the TTCF representation for the N-particle distribution function must be,

$$f(t) = f(0) - \beta\gamma V \int_0^t ds J(-s) f(s) \quad (7.3.12)$$

We can now successively substitute the transient correlation function expression for the nonequilibrium distribution function into the right hand side of (7.3.12). This gives,

$$\begin{aligned} \langle B(t) \rangle &= \int d\Gamma B f(0) - \beta\gamma V \int_0^t ds_1 \int d\Gamma B(0) J(-s_1) f(0) \\ &\quad + (\beta\gamma V)^2 \int_0^t ds_1 \int_0^{s_1} ds_2 \int d\Gamma B(0) J(-s_1) J(-s_2) f(0) + \dots \\ &= \int d\Gamma B(0) \exp\left[-\beta\gamma V \int_0^t ds J(-s)\right] f(0) \end{aligned} \quad (7.3.13)$$

This is precisely the Kawasaki form of the thermostatted nonlinear response. This expression is valid for both the canonical and isokinetic ensembles. It is also valid for the canonical ensemble when the thermostating is carried out using the Nosé-Hoover thermostat.

One can of course also derive the TTCF expression for phase averages from the Kawasaki expression. Following Morriss and Evans, (1985) we simply differentiate the (7.3.13) with respect to time, and then reintegrate.

$$\begin{aligned} \frac{d}{dt} \langle B(t) \rangle &= -\beta\gamma V \int d\Gamma B J(-t) \exp\left[-\beta\gamma V \int_0^t ds J(-s)\right] f(0) \\ &= -\beta\gamma V \int d\Gamma B J(-t) f(t) \\ &= -\beta\gamma V \int d\Gamma B(t) J(0) f(0) \\ &= -\beta\gamma V \langle B(t) J(0) \rangle \end{aligned} \quad (7.3.14)$$

A simple integration of (7.3.14) with respect to time yields the TTCF relation (7.3.8). We have thus proved the formal equivalence of the TTCF and Kawasaki representations for the nonlinear thermostatted response.

Comparing the transient time correlation expression for the nonlinear response with the Kawasaki representation, we see that the difference simply amounts to a time shift. In the transient time correlation form, it is the dissipative flux J , which is evaluated at time zero

whereas in the Kawasaki form, the response variable B , is evaluated at time zero. For equilibrium or steady state time correlation functions the stationarity of averages means that such time shifts are essentially trivial. For transient response correlation functions there is of course no such invariance principle, consequently the time translation transformation is accordingly more complex.

The computation of the time dependent response using the Kawasaki form directly, equation (7.3.13), is very difficult. The inevitable errors associated with the inaccuracy of the trajectory, as well as those associated with the finite grid size in the calculation of the extensive Kawasaki integrand, combine and are magnified by the exponential. This exponential is then multiplied by the phase variable $B(0)$, before the ensemble average performed. In contrast the calculation of the response using the transient correlation expression, equation (7.3.8), is as we shall see, far easier.

It is trivial to see that in the linear regime both the TTCF and Kawasaki expressions reduce to the usual Green-Kubo expressions. The equilibrium time correlation functions that appear in Green-Kubo relations are generated by the field free thermostatted equations. In the TTCF formulae the field is 'turned on' at $t=0$.

The coincidence at small fields, of the Green-Kubo and transient correlation formulae means that unlike direct NEMD, the TTCF method can be used at small fields. This is impossible for direct NEMD because in the small field limit the signal to noise ratio goes to zero. The signal to noise ratio for the transient correlation function method becomes equal to that of the equilibrium Green-Kubo method. The transient correlation function method forms a bridge between the Green-Kubo method which can only be used at equilibrium, and direct NEMD which is the most efficient strong field method. Because a field is required to generate TTCF correlation functions, their calculation using a molecular dynamics, still requires a **nonequilibrium** computer simulation to be performed.

It is also easy to see that at short times there is no difference between the linear and nonlinear stress response. It takes time for the nonlinearities to develop. The way to see this is to expand the transient time correlation function in a power series in γt . The coefficient of the first term in this series is just $V\langle P_{xy}^2 \rangle / k_B T$, the infinite frequency shear modulus, G_∞ . Since this is an equilibrium property its value is unaffected by the strain rate and is thus the same in both the linear and nonlinear cases. If we look at the response of a quantity like the pressure whose linear response is zero, the leading term in the short time expansion is quadratic in the strain rate and in time. The linear response of course is the first to appear.

7.4 Trajectory Mappings.

In calculations of transient time correlation functions it is convenient to generate the initial ensemble of starting states from a single field free, Gaussian isokinetic trajectory. As Gaussian isokinetic dynamics ergodically generates the isokinetic ensemble, a single field free trajectory is sufficient to sample the ensemble. At equally spaced intervals along this single field free trajectory (every N_e timesteps), field dependent simulations are started and followed for N_n timesteps. The number N_n should be greater than the characteristic time required for the system to relax to a steady state and N_e should be large enough to ensure that the initial phases are uncorrelated. Each of these cycles gives one initial phase Γ , for the transient correlation function. This process can be made more efficient if we use this single equilibrium starting state to provide more than one initial phase for the nonequilibrium trajectories. To do this we use a group of phase space mappings.

In this section we develop mappings of the phase, Γ which have useful properties, for the theoretical interpretation and practical implementation of nonlinear response theory. For convenience we shall write the phase, Γ , as $(\mathbf{q}, \mathbf{p}) = (\mathbf{x}, \mathbf{y}, \mathbf{z}, \mathbf{p}_x, \mathbf{p}_y, \mathbf{p}_z)$, where each of the components $\mathbf{x}, \mathbf{y}, \mathbf{z}, \mathbf{p}_x, \mathbf{p}_y, \mathbf{p}_z$ is itself an N -dimensional vector. The time evolution of an arbitrary phase variable $B(\Gamma)$ is governed by the phase variable propagator $\exp(iLt)$, so that $B(t) = B(\Gamma(t)) = \exp(iLt) B(\Gamma)$. Note that the propagator is an operator which acts on the *initial* phases Γ , so in order to calculate the action of the propagator on a phase variable at a time other than zero, $B(t)$ has to be expressed as a function of the initial phases Γ and not the current phases $\Gamma(t)$. We assume that the equations of motion have no explicit time dependence (by way of a time dependent external field). The propagator is therefore a shift operator. In the time dependent case, the propagator is not a simple shift operator and the results which follow will need to be generalised. We leave this generalisation until Chapter 8.

The phase variable B at time t , $B(t)$, can be traced back to time zero by applying the negative-time phase variable propagator $\exp(-iLt)$,

$$\exp(-iLt) B(t) = \exp(-iLt) \exp(iLt) B(\Gamma) = B(\Gamma). \quad (7.4.1)$$

Reversing the sign of the time in the propagator *retraces* the original trajectory. It is possible to *return* to the original phase point $\Gamma(0)$ without changing the sign of the time. This is achieved by mapping the phase point $\Gamma(t)$ so that a combination of positive time evolution and mapping takes $\Gamma(t) \Rightarrow \Gamma(0)$. This mapping is called the time reversal mapping \mathbf{M}^T . For field free equations of motion, this is straightforward as the mapping simply consists of reversing the signs of all the momenta.

$$\mathbf{M}^T(\mathbf{q}, \mathbf{p}) = (\mathbf{q}^T, \mathbf{p}^T) = (\mathbf{q}, -\mathbf{p}). \quad (7.4.2)$$

It is important to realise that this process does not lead to a *retracing* of the original trajectory, as everywhere along the *return* path the momenta are the opposite sign to those of the *forward* path. Noting that $e^{iLt} = e^{iL(\Gamma)t}$, this can be summarised: $\mathbf{M}^T e^{iLt} \mathbf{M}^T e^{iLt} \Gamma(0) = \mathbf{M}^T e^{iLt} \mathbf{M}^T \Gamma(t) = e^{-iLt} \Gamma(t) = \Gamma(0)$. These results will be derived in more detail later.

Given an initial starting phase $\Gamma = (\mathbf{x}, \mathbf{y}, \mathbf{p}_x, \mathbf{p}_y)$ then four starting phases, which occur within the equilibrium distribution with the same probability as Γ , can be obtained using the mappings \mathbf{M}^I , \mathbf{M}^T , \mathbf{M}^Y and \mathbf{M}^K ;

$$\begin{aligned}
 \Gamma^I &= \mathbf{M}^I [\Gamma] &= (\mathbf{x}, \mathbf{y}, \mathbf{z}, \mathbf{p}_x, \mathbf{p}_y, \mathbf{p}_z) \\
 \Gamma^T &= \mathbf{M}^T [\Gamma] &= (\mathbf{x}, \mathbf{y}, \mathbf{z}, -\mathbf{p}_x, -\mathbf{p}_y, -\mathbf{p}_z) \\
 \Gamma^Y &= \mathbf{M}^Y [\Gamma] &= (\mathbf{x}, -\mathbf{y}, \mathbf{z}, \mathbf{p}_x, -\mathbf{p}_y, \mathbf{p}_z) \\
 \Gamma^K &= \mathbf{M}^K [\Gamma] &= (\mathbf{x}, -\mathbf{y}, \mathbf{z}, -\mathbf{p}_x, \mathbf{p}_y, -\mathbf{p}_z).
 \end{aligned}
 \tag{7.4.3}$$

Here \mathbf{M}^I is the identity mapping; \mathbf{M}^T is the time reversal mapping introduced above; \mathbf{M}^Y is termed the y-reflection mapping; and \mathbf{M}^K is called the Kawasaki mapping (it is the combined effect of time reversal and y-reflection mapping $\mathbf{M}^K = \mathbf{M}^T \mathbf{M}^Y$). For shear flow these four configurations give four different starting states, and lead to four different field dependent trajectories from the single equilibrium phase point Γ . Each of the mappings consists of a pair of reflections in a coordinate or momentum axis. In total there are 2^4 states that can be obtained using the reflections of a 2-dimensional phase space however, only 2^3 of these states will result in *at most* a sign change in the instantaneous shear stress $P_{xy}(\Gamma)$. Only 2^2 of the remaining mappings lead to different shearing trajectories. The shear stress obtained from trajectories starting from Γ_i and $-\Gamma_i$ for example, are identical. The probability of each of these states occurring within the equilibrium distribution, is identical because the Hamiltonian H_0 , is invariant under these mappings.

There is a second, more important, advantage of this procedure. If we examine the transient response formula (7.3.7), we see that at long time the correlation function $\langle B(t)P_{xy}(0) \rangle$ approaches $\langle B(\infty) \rangle \langle P_{xy}(0) \rangle$. The steady state average of B is usually non-zero (in contrast to equilibrium time correlation functions). To minimise the statistical uncertainties in calculating the transient correlation integral, it is necessary to choose equilibrium starting states Γ in such a way that $\langle P_{xy}(0) \rangle \equiv 0$. The phase mapping procedure described above achieves this. If the shear stress computed from the original starting phase is P_{xy} , then the shear stress from Γ^T is also equal to P_{xy} , but the shear stresses from both Γ^Y and Γ^K are equal to $-P_{xy}$. This means that the sum of the shear stresses from these four starting phases is **exactly** zero, so if each chosen Γ is mapped in this way the average shear stress is exactly zero regardless of the number of samplings of Γ . The statistical difficulties at long time, associated with a small non-zero value the average of $P_{xy}(0)$, are eliminated.

There are two further operations on these mappings which we need to complete the development of the mapping algebra. First we need to know how each of the mappings affect phase variables. Second we must understand the effect of the mapping on the phase variable Liouvillean $iL(\Gamma)$, as it is also a function of the initial phase point Γ . To do this we need to know how the equations of motion transform. First we will discuss the transformation of Hamiltonian equations of motion under the mapping, and then consider the transformation of the field dependent dynamics. This will require an extension of the mappings to include the field itself.

To illustrate the development we will consider the time reversal mapping \mathbf{M}^T in detail, and simply state the results for other mappings. In what follows the mapping operator \mathbf{M}^T operates on all functions and operators (which depend upon Γ and γ) to its right. A particular example is useful at this stage, so consider the shear stress P_{xy}

$$\begin{aligned} \mathbf{M}^T [P_{xy}] &= \mathbf{M}^T \left[\sum_{i=1}^N \frac{p_{xi}p_{yi}}{m} + \sum_{i=1}^N y_i F_{xi} \right] \\ &= \sum_{i=1}^N \frac{(-p_{xi})(-p_{yi})}{m} + \sum_{i=1}^N y_i F_{xi} \\ &= P_{xy} \end{aligned} \tag{7.4.4}$$

Here P_{xy} is mapped to the same value. For thermodynamically interesting phase variables the operation of the mappings involve simple parity changes

$$\mathbf{M}^X B(\Gamma) = p_B^X B(\Gamma) \tag{7.4.5}$$

where $p_B^X = \pm 1$. In the following table we list the values of the parity operators for shear stress, pressure and energy for each of the mappings.

Table 7.1 Mapping Parities

Parity Operators	Mapping	shear stress	pressure	energy
\mathbf{M}^I	Identity	1	1	1
\mathbf{M}^T	Time reversal	1	1	1
\mathbf{M}^Y	y-reflection	-1	1	1
\mathbf{M}^K	Kawasaki	-1	1	1

The operation of the mapping \mathbf{M}^T on the Hamiltonian equations of motion is

$$\mathbf{M}^T \dot{\mathbf{q}}_i = \mathbf{M}^T \left[\frac{\mathbf{p}_i}{m} \right] = \frac{\mathbf{p}_i^T}{m} = \frac{-\mathbf{p}_i}{m} = -\dot{\mathbf{q}}_i \quad (7.4.6)$$

$$\mathbf{M}^T \dot{\mathbf{p}}_i = \mathbf{M}^T [\mathbf{F}_i(\mathbf{q})] = \mathbf{F}_i(\mathbf{q}^T) = \mathbf{F}_i(\mathbf{q}) = \dot{\mathbf{p}}_i \quad (7.4.7)$$

where the transformed coordinate and momenta are denoted by the superscript (T). The vector character of the force \mathbf{F} is determined by the coordinate vector \mathbf{q} , so that under this mapping the force is invariant. Because $d\mathbf{q}/dt$ and \mathbf{p} change sign under the mapping \mathbf{M}^T , the phase variable Liouvillean becomes

$$\begin{aligned} \mathbf{M}^T iL(\Gamma) &= \mathbf{M}^T \left[\dot{\Gamma} \cdot \frac{\partial}{\partial \Gamma} \right] = \mathbf{M}^T \left[\sum_{i=1}^N (\dot{\mathbf{q}}_i \cdot \frac{\partial}{\partial \mathbf{q}_i} + \dot{\mathbf{p}}_i \cdot \frac{\partial}{\partial \mathbf{p}_i}) \right] \\ &= \sum_{i=1}^N (\dot{\mathbf{q}}_i^T \cdot \frac{\partial}{\partial \mathbf{q}_i^T} + \dot{\mathbf{p}}_i^T \cdot \frac{\partial}{\partial \mathbf{p}_i^T}) \\ &= \sum_{i=1}^N (-\dot{\mathbf{q}}_i \cdot \frac{\partial}{\partial \mathbf{q}_i} + \dot{\mathbf{p}}_i \cdot \frac{\partial}{\partial (-\mathbf{p}_i)}) = -iL(\Gamma) \end{aligned} \quad (7.4.8)$$

It is straightforward to use this result and the series expansion of the propagator to show that

$$\mathbf{M}^T \exp(iL(\Gamma)t) = \exp(-iL(\Gamma)t) \quad (7.4.9)$$

To see exactly how this combination of the \mathbf{M}^T mapping, and forward time propagation combine to give time reversal we consider the time evolution of Γ itself,

$$\begin{aligned} \Gamma &= \exp(-iL(\Gamma)t) \exp(iL(\Gamma)t) \Gamma \\ &= \mathbf{M}^T \mathbf{M}^T \exp(-iL(\Gamma)t) \exp(iL(\Gamma)t) \Gamma \\ &= \mathbf{M}^T \exp(\mathbf{M}^T [-iL(\Gamma)] t) \mathbf{M}^T \exp(iL(\Gamma)t) \Gamma \\ &= \mathbf{M}^T \exp(iL(\Gamma)t) \mathbf{M}^T \exp(iL(\Gamma)t) \Gamma \end{aligned} \quad (7.4.10)$$

This implies that

$$\mathbf{M}^T \exp(iL(\Gamma)t) \mathbf{M}^T \exp(iL(\Gamma)t) = \mathbf{1}. \quad (7.4.11)$$

If we start with $\Gamma(0)$, propagate forward to time t , map with \mathbf{M}^T (changing the signs of the

momenta), propagate forward to time t , and map with \mathbf{M}^T (changing the signs of the momenta again), we return to $\Gamma(0)$. An analogous identity can be constructed by considering $\Gamma(0) = \exp(iL(\Gamma)t) \Gamma(-t)$, that is

$$\mathbf{M}^T \exp(-iL(\Gamma)t) \mathbf{M}^T \exp(-iL(\Gamma)t) = \mathbf{1}. \quad (7.4.12)$$

This says that we can complete a similar cycle using the backward time propagator $\exp(-iLt)$ first. These two results demonstrate the various uses of this time reversal mapping.

When the equations of motion for the system involve an external field the time reversal mapping can be generalised to include the field. This is necessary if we wish to determine whether a particular mapping leads to different field dependent dynamics. Here we limit consideration to the isothermal SLLOD algorithm for shear flow. It is clear that all the momenta must change sign so a suitable choice for the mapping is

$$\mathbf{M}^T(\mathbf{q}, \mathbf{p}, \gamma) = (\mathbf{q}, -\mathbf{p}, -\gamma). \quad (7.4.13)$$

As the field has units of inverse time the field changes sign together with the momenta. The equations of motion for the mapped variables become

$$\begin{aligned} \mathbf{M}^T \dot{\mathbf{q}}_i &= \mathbf{M}^T \left[\frac{\mathbf{p}_i}{m} + \mathbf{n}_x \gamma y_i \right] \\ &= \frac{\mathbf{p}_i}{m} + \mathbf{n}_x \gamma^T y_i^T \\ &= \frac{-\mathbf{p}_i}{m} + \mathbf{n}_x (-\gamma) y_i \\ &= -\dot{\mathbf{q}}_i \end{aligned} \quad (7.4.14)$$

and

$$\begin{aligned} \mathbf{M}^T \dot{\mathbf{p}}_i &= \mathbf{M}^T [\mathbf{F}_i(\mathbf{q}) - \mathbf{n}_x \gamma p_{yi} - \alpha \mathbf{p}_i] \\ &= \mathbf{F}_i(\mathbf{q}^T) - \mathbf{n}_x \gamma^T p_{yi}^T - \alpha^T \mathbf{p}_i^T \\ &= \mathbf{F}_i(\mathbf{q}) - \mathbf{n}_x (-\gamma) (-p_{yi}) - (-\alpha) (-\mathbf{p}_i) \\ &= \mathbf{F}_i(\mathbf{q}) - \mathbf{n}_x \gamma p_{yi} - \alpha \mathbf{p}_i \\ &= \dot{\mathbf{p}}_i \end{aligned} \quad (7.4.15)$$

Notice also that for the thermostating variable α

$$\alpha^T = \mathbf{M}^T \alpha = \mathbf{M}^T \left[\frac{\sum_{i=1}^N (\mathbf{F}_i \cdot \mathbf{p}_i - \gamma p_{xi} p_{yi})}{\sum_{i=1}^N p_i^2} \right] = -\alpha \quad (7.4.16)$$

as the numerator changes sign and the denominator is invariant under the time reversal mapping. The mapping of the Liouvillean is similar to the field free case and it can be shown that

$$\mathbf{M}^T iL(\Gamma, \gamma) = -iL(\Gamma, -\gamma) \quad (7.4.17)$$

In the field dependent case the two operators, equations (7.4.11,7.4.12) generalise to

$$\mathbf{M}^T \exp(iL(\Gamma, -\gamma)t) \mathbf{M}^T \exp(iL(\Gamma, \gamma)t) = \mathbf{1}. \quad (7.4.18)$$

$$\mathbf{M}^T \exp(-iL(\Gamma, -\gamma)t) \mathbf{M}^T \exp(-iL(\Gamma, \gamma)t) = \mathbf{1}. \quad (7.4.19)$$

As a phase variable by definition is not a function of the field, the parity operators associated with mapping phase variables are unchanged.

The second mapping we consider is the y-reflection mapping \mathbf{M}^Y , as it acts to change the sign of the shear rate but not the time or the Liouvillean. This mapping is defined by

$$\mathbf{M}^Y(\mathbf{x}, \mathbf{y}, \mathbf{z}, \mathbf{p}_x, \mathbf{p}_y, \mathbf{p}_z, \gamma) = (\mathbf{x}, -\mathbf{y}, \mathbf{z}, \mathbf{p}_x, -\mathbf{p}_y, \mathbf{p}_z, -\gamma) \quad (7.4.20)$$

This mapping consists of a coordinate reflection in the \mathbf{x}, \mathbf{z} -plane, and momenta reflection in the $\mathbf{p}_x, \mathbf{p}_z$ -plane. Substituting this mapping into the SLLOD equations of motion shows that the time derivatives of both \mathbf{y} and \mathbf{p}_y change sign, while the thermostating variable remains unchanged. The y-reflection Liouvillean is related to the standard Liouvillean by

$$\mathbf{M}^Y iL(\Gamma, \gamma) = iL(\Gamma, -\gamma) \quad (7.4.21)$$

We now define the combination Kawasaki mapping \mathbf{M}^K , which consists of the time reversal mapping followed by the y reflection mapping, so that

$$\mathbf{M}^K(\mathbf{x}, \mathbf{y}, \mathbf{z}, \mathbf{p}_x, \mathbf{p}_y, \mathbf{p}_z, \gamma) = (\mathbf{x}, -\mathbf{y}, \mathbf{z}, -\mathbf{p}_x, \mathbf{p}_y, -\mathbf{p}_z, \gamma) \quad (7.4.22)$$

$$-\beta \int_0^t ds \gamma P_{xy}(-s, \gamma, \Gamma) V$$

using the Kawasaki mapping the negative time evolution can be transformed to an equivalent positive time evolution. To do this consider

$$\begin{aligned} P_{xy}(-s, \Gamma, \gamma) &= \exp(-iL(\Gamma, \gamma) s) P_{xy}(\Gamma) \\ &= \exp(iL(\Gamma^K, \gamma^K) s) p_{P_{xy}} P_{xy}(\Gamma^K) \\ &= - \exp(iL(\Gamma^K, \gamma^K) s) P_{xy}(\Gamma^K) \\ &= - P_{xy}(s, \Gamma^K, \gamma^K) \\ &= - P_{xy}(s, \Gamma^K, \gamma) \end{aligned} \tag{7.4.25}$$

The last equality follows from the fact that $\gamma^K = \gamma$. So we may think of $P_{xy}(-s, \gamma, \Gamma)$ as equivalent (apart from the sign of the parity operator) to the propagation of P_{xy} forward in time, with the same γ , but starting from a different phase point Γ^K . The probability of this new phase point Γ^K in the canonical (or isothermal) distribution is the same as the original Γ , as the equilibrium Hamiltonian H_0 , is invariant under time reversal and reflection. Therefore the Kawasaki distribution function can be written as

$$\begin{aligned} f(\Gamma, t) &= \exp\left[-\beta\gamma V \int_0^t ds P_{xy}(-s, \Gamma, \gamma)\right] f(0, \Gamma, 0) \\ &= \exp\left[+\beta\gamma V \int_0^t ds P_{xy}(+s, \Gamma^K, \gamma)\right] f(0, \Gamma^K, 0) \end{aligned} \tag{7.4.26}$$

In this form the sign of the exponent itself changes as well as the sign of the time evolution. At sufficiently large time $P_{xy}(s, \Gamma^K, \gamma)$ approaches the steady state value $\langle P_{xy}(s, \gamma) \rangle$, regardless of the initial phase point Γ^K .

7.5 Numerical Results for the Transient Time Correlation Function.

Computer simulations have been carried out for two different systems (Evans and Morriss, 1988). Two statistical mechanical systems were studied. The first was a system of 72 soft disks, ($\phi=4\epsilon(\sigma/r)^{12}$), in two dimensions at a reduced density, $\rho^*=\rho\sigma^2 = 0.6928$, a reduced temperature, $T^* = kT/\epsilon = 1$, and for a range of reduced strain rates, $\gamma^* = \gamma(m/\epsilon)^{1/2}\sigma = \partial u_x/\partial y (m/\epsilon)^{1/2}\sigma$. The second system was studied more extensively. It consisted of 256 WCA particles. The system was three dimensional and the density was set to $\rho^*=\rho\sigma^3 = 0.8442$ while the temperature was $T^* = kT/\epsilon = 0.722$ (ie the Lennard-Jones triple point state).

In each simulation the direct NEMD average of the shear stress, pressure, normal stress difference and thermostat multiplier α , were calculated along with their associated transient correlation functions using typically 60,000 nonequilibrium starting states. For the three dimensional system each nonequilibrium trajectory was run for a reduced time of 1.5 (600 timesteps). Each 60,000 starting state simulation consisted of a total of 54 million timesteps made up of $2 \times 15,000 \times 600$ timesteps at equilibrium and $4 \times 15,000 \times 600$ perturbed nonequilibrium timesteps. The trajectory mappings described in §7.4 were used to generate the 4 starting states for the nonequilibrium trajectories.

In Figure 7.1 we present the results obtained for the reduced shear stress $P_{xy}^*=P_{xy}(\sigma^2/\epsilon)$, in the 2 dimensional soft disk system. The imposed reduced strain rate is unity. The values of the shear stress calculated from the transient correlation function expression, $(P_{xy}(T))$, agree within error bars, with those calculated directly, $(P_{xy}(D))$. The errors associated with the direct average are less than the size of the plotting symbols whereas the error in the integral of the transient correlation function is approximately $\pm 2.5\%$ at the longest times. Although the agreement between the direct simulation results and the TTCF prediction is very good it must be remembered that the total response for the shear stress is the sum of a large linear effect which could be correctly predicted by the Green-Kubo formula and a smaller ($\sim 25\%$) nonlinear effect. Thus the statistical agreement regarding the TTCF prediction of the intrinsically nonlinear component of the total response is therefore approximately 10%.

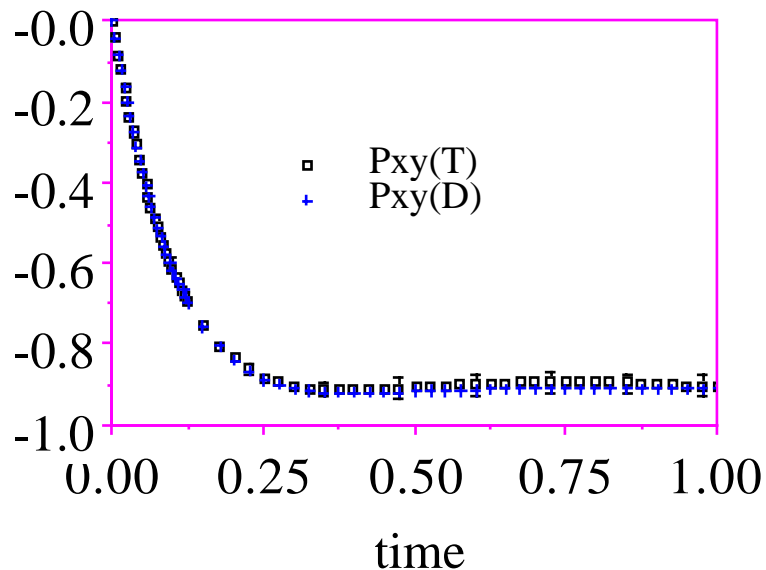


Figure 7.1

The shear-induced increase in pressure with increasing strain rate (shear dilatancy) is an intrinsically nonlinear effect and is not observed in Newtonian fluids. The Green-Kubo formulae predict that there is no coupling of the pressure and the shear stress because the equilibrium correlation function, $\langle \Delta p(t) P_{xy}(0) \rangle$, is exactly zero at all times. In Figure 7.2 we present the direct and transient correlation function values of the difference between the pressure $p^* = p(\sigma^2/\varepsilon)$ and its equilibrium value, p_0^* , ($\Delta p^* = p^* - p_0^*$). The agreement between the direct average, and the value obtained from the transient correlation function expression at $\gamma^* = 1.0$ is impressive. It is important to note that the agreement between theory and simulation shown in Figure 7.2, is a test of the predictions of the theory for an *entirely* nonlinear effect. It is a more convincing check on the validity of the TTCF formalism than are the results for the shear stress because there is no underlying linear effect.

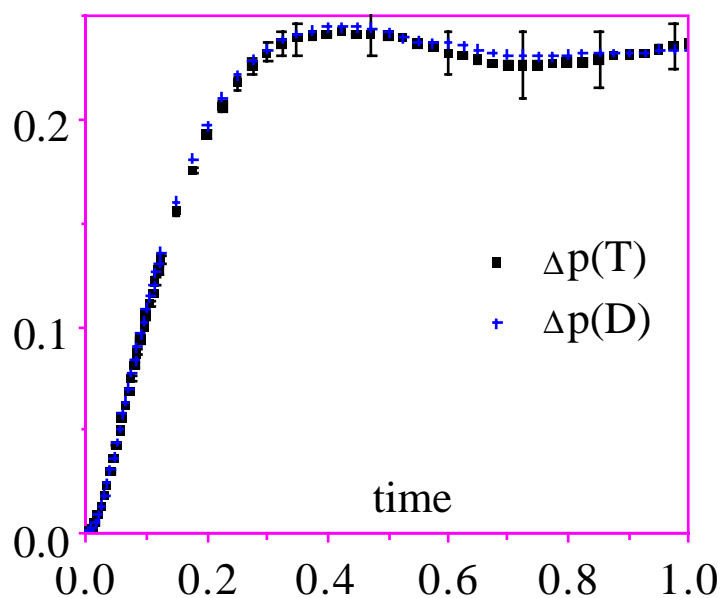
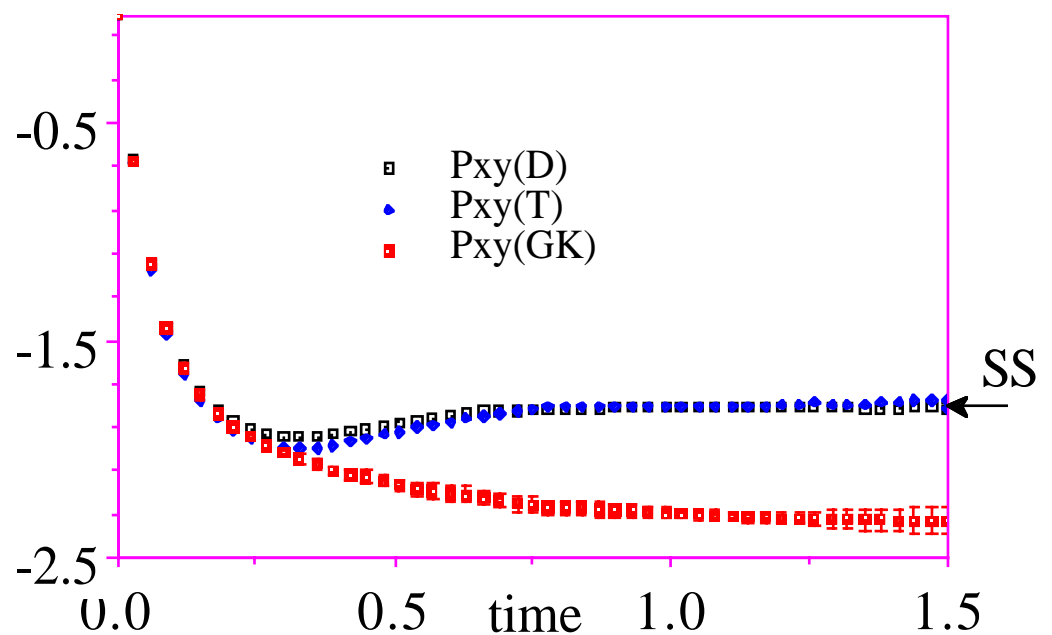


Figure 7.2

The results for the x-y element of the pressure tensor in the three dimensional WCA system are given in Figure 7.3. Again the agreement between the TTCF prediction (T), and the Direct simulation (D), is excellent. We also show the long time steady state stress computed by conventional NEMD (denoted, SS). It is clear that our time limit for the integration of the Transient Time Correlation Functions is sufficient to obtain convergence of the integrals (i.e. to ensure relaxation to the nonequilibrium steady state). We also show the Green-Kubo prediction for the stress (GK). A comparison of the linear and nonlinear responses shows that the intrinsically nonlinear response is only generated at comparatively late times. The response is essentially linear until the stress overshoot time ($t^* \sim 0.3$). The figure also shows that the total nonlinear response converges far more rapidly than does the linear GK response. The linear GK response has obviously not relaxed to its steady state limiting value at a t^* value of 1.5. This is presumably because of long time tail effects which predict that the linear response relaxes very slowly as $t^{-1/2}$, at long times.

**Figure 7.3**

In Figure 7.4 we show the corresponding results for shear dilatancy in three dimensions. Again the TTCF predictions are in statistical agreement with the results from direct simulation. We also show the steady state pressure shift obtained using conventional NEMD. Again it is apparent that $t^* = 1.5$ is sufficient to obtain convergence of the TTCF integral. Although it is not easy to see in the figure, the initial slope of the pressure response is zero.

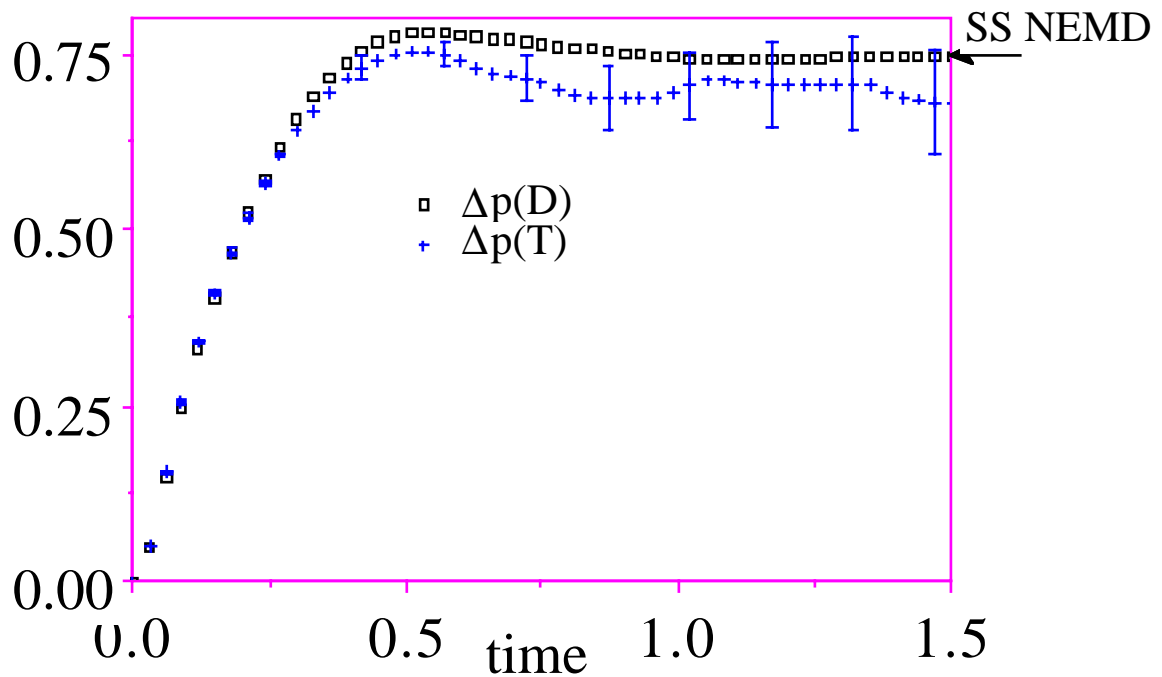


Figure 7.4

This contrasts with the initial slope of the shear stress response which is G_∞ . This is in agreement with the predictions of the transient time correlation formalism made in §7.3. Figures 7.1,7.3 clearly show that at short time the stress is controlled by linear response mechanisms. It takes time for the nonlinearities to develop but paradoxically perhaps, convergence to the steady state asymptotic values is ultimately much faster in the nonlinear, large field regime.

Comparing the statistical uncertainties of the transient correlation and direct NEMD results shows that at reduced strain rates of unity conventional NEMD is clearly the most efficient means of establishing the steady state response. For example under precisely the same conditions: after 54 million timesteps the TTCF expression for P_{xy} is accurate to $\pm 0.05\%$, but the directly averaged transient response is accurate to $\pm 0.001\%$. Because time is not wasted in establishing the steady state from each of 60,000 time origins, conventional steady state NEMD needs only 120 thousand timesteps to obtain an uncertainty of $\pm 0.0017\%$. If we assume that errors are inversely proportional to the square root of the run length, then the relative uncertainties for a 54 million timestep run would be $\pm 0.05\%$, $\pm 0.001\%$ and 0.00008% for the TTCF, the directly averaged transient response and for conventional NEMD, respectively. Steady state NEMD is about 600 times more accurate than TTCF for the same number of timesteps. On the other hand, the transient correlation method has a computational efficiency which is similar to that of the equilibrium Green-Kubo method. For TTCFs time origins cannot be taken more frequently than the time interval over which the TTCFs are calculated. An advantage of the TTCF formalism is that it models the rheological problem of stress growth (Bird et. al., 1977), not simply steady shear flow, and we can observe the associated effects such as stress overshoot, and the time development of normal stress differences.

Figure 7.5 shows the transient responses for the normal stress differences, $P_{yy}-P_{zz}$ and $P_{xx}-P_{yy}$, for the three dimensional WCA system at a reduced strain rate of unity. The normal stress differences are clearly more subtle than either the shear stress or the hydrostatic pressure. Whereas the latter two functions seem to exhibit a simple overshoot before relaxing to their final steady state values, the normal stress differences show two maxima before achieving their steady state values (indicated SS, in the figure). As before it is apparent that $t^* = 1.5$, is sufficient time for an essentially complete relaxation to the steady state.

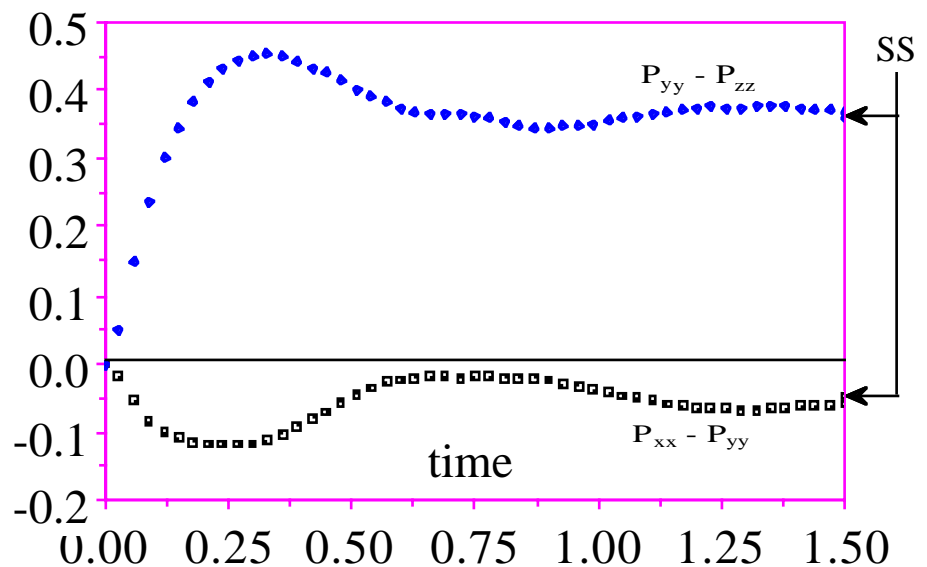


Figure 7.5

Over the years a number of numerical comparisons have been made between the Green-Kubo expressions and the results of NEMD simulations. The work we have just described takes this comparison one step further. It compares NEMD simulation results with the thermostatted, nonlinear generalisation of the Green-Kubo formulae. It provides convincing numerical evidence for the usefulness and correctness of the Transient Time Correlation Function formalism. The TTCF formalism is the natural thermostatted, nonlinear generalisation of the Green-Kubo relations.

7.6 Differential Response Functions.

Surprisingly often we are interested in the intermediate regime where the Green-Kubo method cannot be applied and where, because of noise, direct NEMD is very inefficient. We have just seen how the TTCF method may be applied to strong fields. It is also the most efficient known method for treating fields of intermediate strength. Before we demonstrate the application of TTCFs to the small field response, we will describe an early method that was used to calculate the intermediate field response.

Prior to the development of Transient Time Correlation Function method, the only way of computing the small but finite field response of many-body systems was to use the Subtraction or Differential response method. The idea behind this method is extremely simple. By considering a sufficiently small field, the systematic response (ie the field induced response) will be swamped by the natural (essentially equilibrium) fluctuations in the system. However it is clear that for short times and small applied fields, there will be a high degree of correlation in the transient response computed with, and without, the external field, (see Figure 7.6).

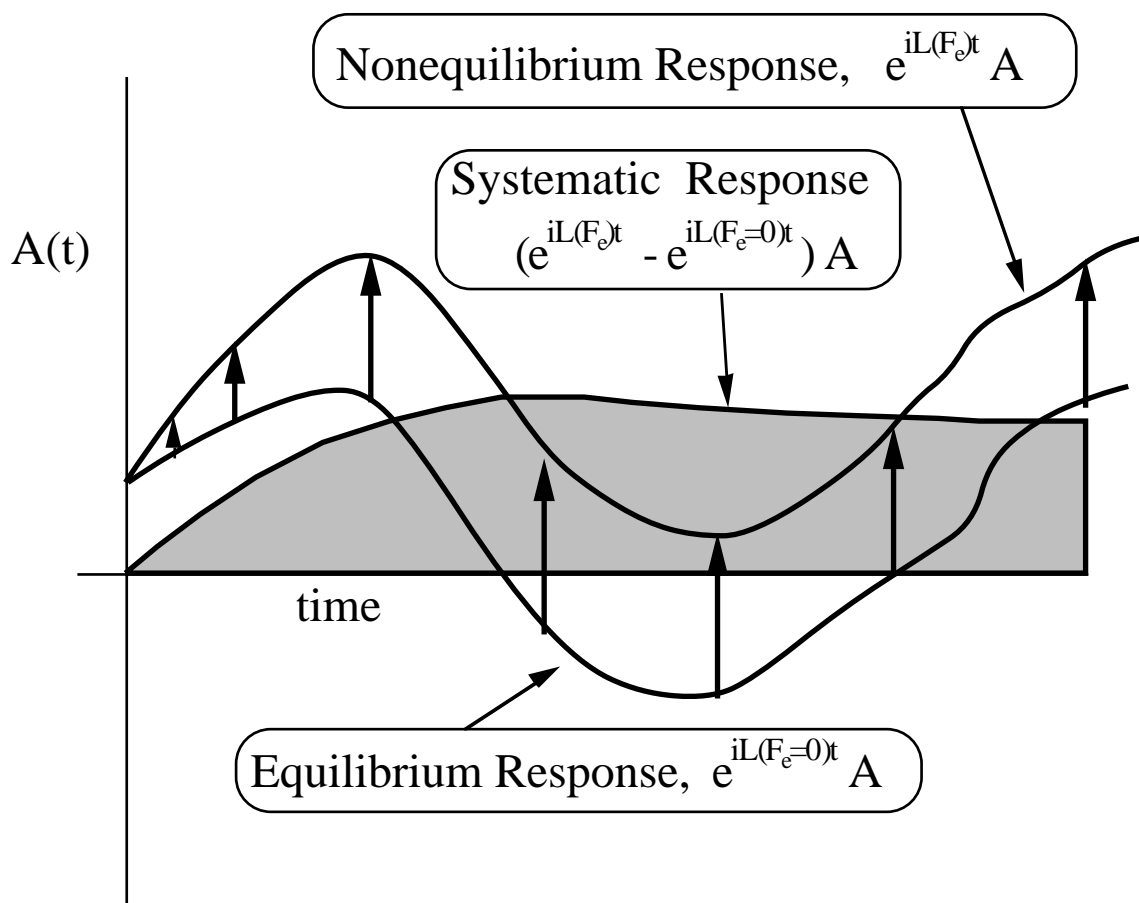


Figure 7.6

If we compute $A(t)$ for two trajectories which start at the same phase, Γ , one with the field on and the other with the field off, we might see what is depicted in Figure 7.6. Ciccotti et. al. (1975, 1976, 1979), realised that, for short times, the noise in $A(t)$ computed for the two trajectories, will be highly correlated. They used this idea to reduce the noise in the response

computed at small applied fields.

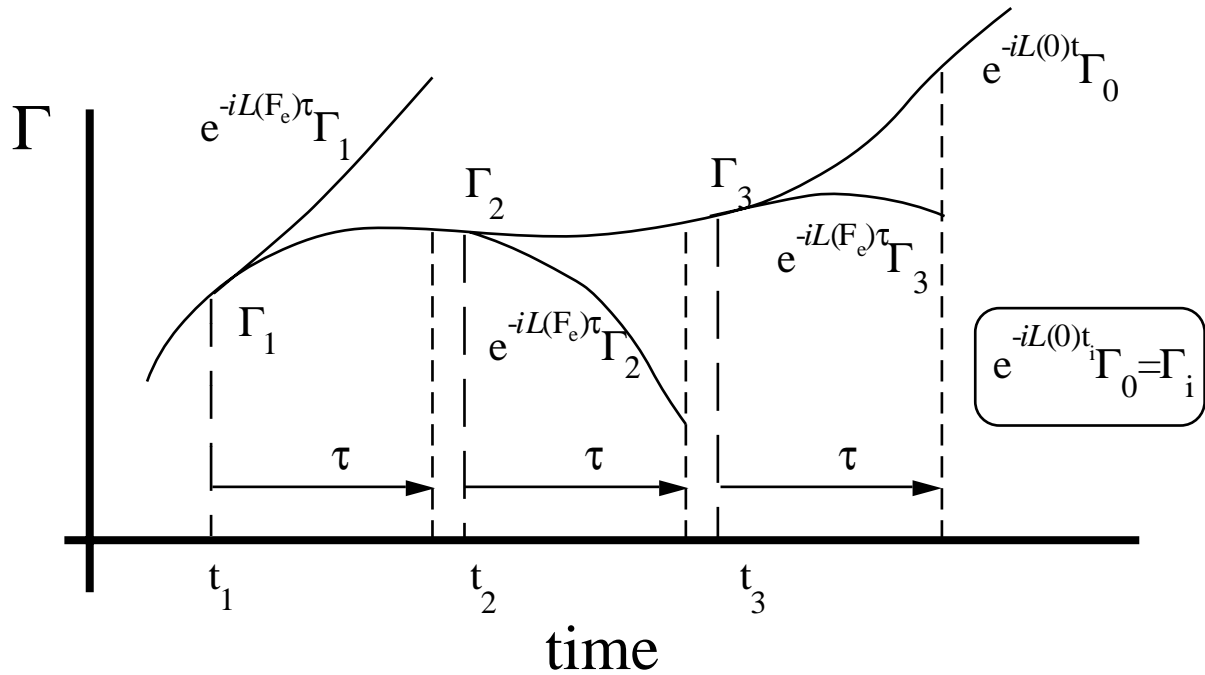


Figure 7.7

To use their *Subtraction Method* one performs an equilibrium simulation ($F_e=0$), from which one periodically initiates nonequilibrium calculations ($F_e \neq 0$). The general idea is shown in Figure 7.7. The phases $\{\Gamma_i\}$, are taken as time origins from which one calculates the differences of the response in a phase variable with and without the applied field. The *systematic* or nonequilibrium response is calculated from the equation,

$$\langle A(t;F_e) \rangle = \langle A(t;F_e) \rangle - \langle A(t;0) \rangle = \frac{1}{N} \sum_{i=1}^N [e^{iL(F_e)t} - e^{iL(0)t}] A(\Gamma_i) \quad (7.6.1)$$

For many years this was the only method of calculating the small field nonequilibrium response. It suffers from a major problem however. For the method to work, the noise in the the value of $A(t)$ computed with and without the field, must be highly correlated. Otherwise the equilibrium fluctuations will completely swamp the desired response. Now the noise in the two responses will only be correlated if the two systems remain sufficiently close in phase space. The Lyapunov instability (§3.4) will work against this. The Lyapunov instability will try to drive the two systems apart exponentially fast. This can be expected to lead to an exponential growth of noise with respect to time. This is illustrated in Figures 7.8,9 in which the TCF, denoted (T), and Subtraction techniques, denoted (sub), are compared for the 256 particle WCA system considered in §7.5.

Figure 7.8 shows the shear stress for the three dimensional WCA system at the comparatively small strain rate of $\dot{\gamma}^* = 10^{-3}$. At this field strength conventional steady state NEMD is swamped by noise. However the Subtraction technique can be used to substantially

improve the statistics. It is important to note that both the Subtraction and TTCF technique are based on an analysis of the transient response of systems. The results compared in Figure 7.8 were computed for **exactly** the same system using **exactly** the same data. The only difference between the two sets of results is how the data were analysed. Lyapunov noise is clearly evident in the Subtraction results labelled in Figure 7.8 as $P_{xy}(\text{sub})$. For longer times, during which we expect the slow nonlinearities to complete the relaxation to the steady state, the Subtraction technique becomes very noisy.

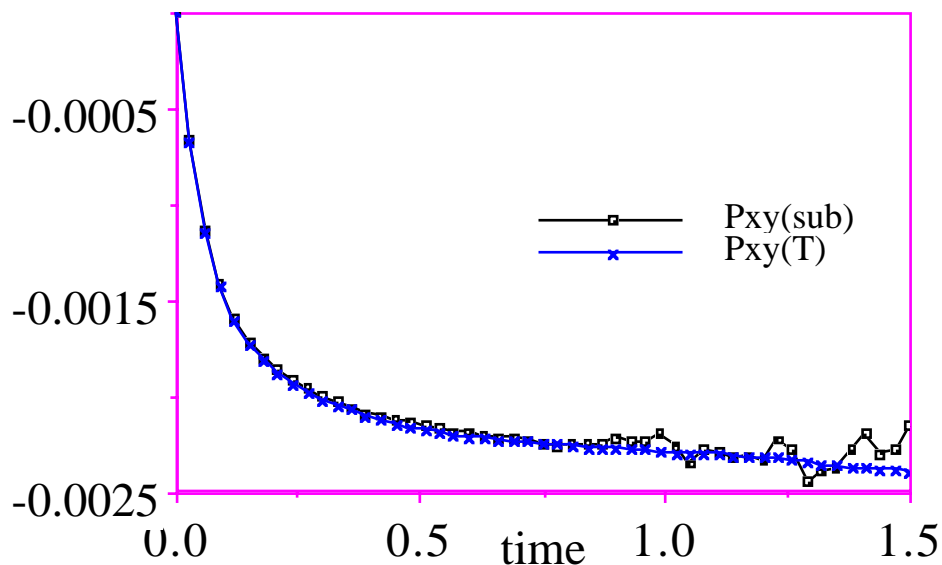


Figure 7.8

Figure 7.9 shows the corresponding results for shear dilatancy. Here the Subtraction technique (labelled 'sub'), is essentially useless. Even the TTCF method becomes somewhat noisy at long times. The TTCF results clearly show the existence of a measurable, intrinsically nonlinear effect even at this small strain rate.

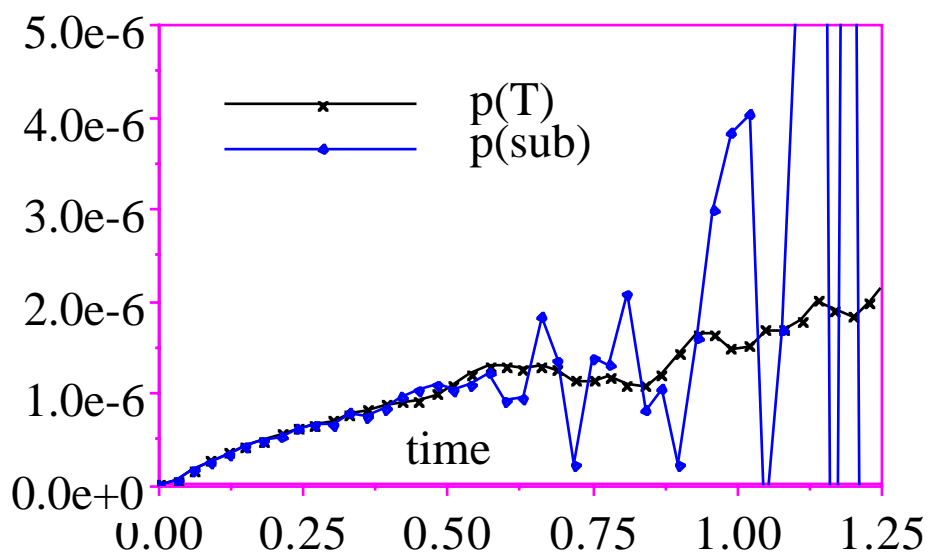


Figure 7.9

Although the TTCF method allows us to compute the response of systems to fields

of arbitrary, even zero, strength, we often require more information about the small field response than it is capable of providing. For example at small fields the response is essentially linear. Nonlinear effects that we may be interested in are completely swamped by the linear response terms. The *Differential Transient Time Correlation Function* (DTTCF) is an attempt to provide an answer to this problem. It uses a subtraction technique on the TTCFs themselves to formally subtract the linear response.

In the DTTCF method we consider the difference between $B(s)$ evaluated with and without the external field, starting from the same initial phase point. From the transient correlation function expression this gives

$$\begin{aligned} \langle B(t, \gamma) - B(0, \gamma) \rangle &= -\beta \mathcal{W} \int_0^t ds \langle (B(s, \gamma) - B(s, 0) + B(s, 0)) P_{xy} \rangle \\ &= -\beta \mathcal{W} \int_0^t ds \langle (B(s, \gamma) - B(s, 0)) P_{xy} \rangle + \beta \mathcal{W} \int_0^t ds \langle B(s, 0) P_{xy} \rangle \end{aligned} \quad (7.6.2)$$

In this equation $B(s, \gamma)$ is generated from $B(0)$ by the thermostatted field dependent propagator. $B(s, 0)$, on the other hand is generated by the zero-field thermostatted propagator. The last term is the integral of an equilibrium time correlation function. This integral is easily recognised as the **linear**, Green-Kubo response. The first term on the RHS is the integral of a differential transient time correlation function (DTTCF), and is the intrinsically nonlinear response. The LHS is termed the direct differential, or subtraction average.

There are two possible cases; the first in which B has a non-zero linear response term, and the second where the linear response is identically zero. If B is chosen to be P_{xy} the third term in (7.6.2) is the Green-Kubo expression for the response of the shear stress $-\eta(0)\gamma$, where $\eta(0)$ is the zero shear rate shear viscosity. The definition of the shear rate dependent viscosity, $\eta(\gamma) \equiv -\langle P_{xy} \rangle / \gamma$ gives

$$\eta(\gamma) - \eta(0) = \beta V \int_0^\infty ds \langle (P_{xy}(s, \gamma) - P_{xy}(s, 0)) P_{xy} \rangle \quad (7.6.3)$$

as the intrinsically nonlinear part of the shear viscosity. As $s \rightarrow \infty$ the differential transient time correlation function (using the mixing assumption) becomes $\langle (P_{xy}(s, \gamma) - P_{xy}(s, 0)) \rangle \langle P_{xy} \rangle = \langle P_{xy}(s, \gamma) \rangle \langle P_{xy} \rangle$. This is zero because $\langle P_{xy}(0) \rangle$ is zero. On the other hand $\langle P_{xy}(s, \gamma) \rangle$ is clearly non-zero which means that the use of our trajectory mappings will improve the statistics as $s \rightarrow \infty$.

To apply the phase space mappings in the differential response method we consider

the identity (7.4.24). We can obtain four different time evolutions of $B(\Gamma)$ by simply removing the minus signs and parity operators from each of the equivalent forms in equation (7.4.24). If we use the index α to denote the 4 mappings $\{I, T, Y, K\}$, then

$$\begin{aligned}
 \sum_{\alpha = \{I, T, Y, K\}} B(t, \Gamma^\alpha, \gamma^\alpha) &= \sum_{\alpha} \exp(iL(\Gamma^\alpha, \gamma^\alpha)t) B(\Gamma^\alpha) \\
 &= \sum_{\alpha} \exp(M^\alpha [iL(\Gamma, \gamma)] t) p_B^\alpha B(\Gamma) \\
 &= \left\{ \exp(iL(\Gamma, \gamma)t) p_B^I + \exp(-iL(\Gamma, -\gamma)t) p_B^T \right. \\
 &\quad \left. \exp(iL(\Gamma, -\gamma)t) p_B^Y + \exp(-iL(\Gamma, \gamma)t) p_B^K \right\} B(\Gamma) \quad (7.6.4)
 \end{aligned}$$

This is the direct response of the phase variable $B(\Gamma)$ from one sampling of Γ , where the mappings are used to generate four starting phase points. To calculate the differential response of B we need to subtract the field free time evolution of $B(\Gamma)$ from each of these four starting states. The four field free time evolutions are found by setting $\gamma^\alpha=0$ in equation (7.6.4). That is

$$\begin{aligned}
 \sum_{\alpha = \{I, T, Y, K\}} B(t, \Gamma^\alpha, \gamma^\alpha=0) &= \left\{ p_B^I \exp(iLt) + p_B^T \exp(-iLt) \right. \\
 &\quad \left. + p_B^Y \exp(iLt) + p_B^K \exp(-iLt) \right\} B(\Gamma) \quad (7.6.5)
 \end{aligned}$$

Clearly there are only two different field free time evolutions; the remaining two can be obtained from these by the sign changes of the parity operators. In practice, a single cycle of the numerical evaluation of a differential transient time correlation function will involve the calculation of four field dependent trajectories and two field free trajectories, yielding four starting states.

The use of the symmetry mappings implies some redundancies in the various methods of calculating the response. In particular the *direct* response of $P_{xy}(t)$ is exactly equal to the *direct differential* response for all values of the time. This means that the contribution from the field free time evolutions is exactly equal to zero. This is easy to see from equation (7.6.4) as there are only two different time evolutions; those corresponding to $\exp(iLt)$ and $\exp(-iLt)$ respectively, and for P_{xy} each comes with a positive and negative parity operator. Therefore these two responses exactly cancel for all values of time.

The second redundancy of interest is that the *transient* response of the pressure $p(t)$ is exactly equal to the *differential transient* response for all values of time. This implies that the contribution to the *equilibrium* time correlation function $\langle p(t) P_{xy} \rangle$ from a single sampling of Γ is exactly zero. Clearly this equilibrium time correlation is zero when the full ensemble average is taken, but the result we prove here is that the mappings ensure that $\sum p(t) P_{xy}$ is zero

for each starting state Γ for all values of t . The contribution from the field free trajectories is

$$\begin{aligned} \sum_{\alpha = \{I, T, Y, K\}} p(t, \Gamma^\alpha, \gamma^\alpha=0) P_{xy}(\Gamma^\alpha) &= P_{xy}(\Gamma) \left\{ p_{P_{xy}}^I p_p^I \exp(iLt) + p_{P_{xy}}^T p_p^T \exp(-iLt) \right. \\ &\quad \left. + p_{P_{xy}}^Y p_p^Y \exp(iLt) + p_{P_{xy}}^K p_p^K \exp(-iLt) \right\} p(\Gamma) \\ &= 0 \end{aligned} \tag{7.6.6}$$

Again the product of parities ensures that the two field free time evolutions $\exp(iLt)$, and $\exp(-iLt)$ occur in cancelling pairs. Therefore the field free contribution to the differential time correlation function is exactly zero and the differential transient results are identical the transient correlation function results.

The DTTCF method suffers from the same Lyapunov noise characteristic of all differential or subtraction methods. In spite of this problem Evans and Morriss (1987) were able to show, using the DTTCF method, that the intrinsically nonlinear response of 3-dimensional fluids undergoing shear flow is given by the classical Burnett form (see §9.5). This is at variance with the nonclassical behaviour predicted by mode coupling theory. However, nonclassical behaviour can only be expected in the large system limit. The classical behaviour observed by Morriss and Evans (1987), is presumably the small strain rate, asymptotic response for **finite** periodic systems.

A much better approach to calculating and analysing the asymptotic nonlinear response will be discussed in §9.5.

7.7 Numerical results for the Kawasaki Representation

We now present results of a direct numerical test the Kawasaki representation of the nonlinear isothermal response. We show that phase averages calculated using the explicitly normalised Kawasaki distribution function agree with those calculated directly from computer simulation.

The system we consider is the thermostatted NEMD simulation of planar Couette flow using the isothermal SLLOD algorithm (§6.3). As remarked earlier, the primary difficulty in using the Kawasaki expression in numerical calculations arises because it involves calculating an extensive exponential. For a 100-particle Lennard-Jones triple point system we would have to average quantities of the order of, e^{200} , to determine the viscosity. Larger system sizes would involve proportionately larger exponents! The simulations presented here attempt to reduce these difficulties by using two strategies: they use a comparatively small number of particles, $N=18$ in two dimensions, and they were carried out at a low density, $\rho^*=0.1$, where the viscosity is ~ 50 times smaller than its triple point value. For small systems it is necessary to take into consideration terms of order, $1/N$, in the definition of the temperature, $T = (\sum_i p_i^2/m) / (dN-d-1)$, and the shear stress, $P_{xy} = \frac{1}{V} \frac{dN-d}{dN-d-1} \sum_i p_{xi} p_{yi} / m - (1/2) \sum_{ij} y_{ij} F_{xij}$.

The first order equations of motion were solved using the 4th order Runge-Kutta method with a reduced timestep of 0.005. The reduced shear rate $\gamma^* = 1$, and the reduced temperature was also set to unity.

The simulation consisted of a single equilibrium trajectory. At regular intervals (every 399 timesteps) the current configuration was used to construct four different configurations using the trajectory mappings described in §7.4. Each of these configurations was used as an initial starting point for a non-equilibrium simulation of 400 timesteps, with a negative timestep and reduced shear rate $\gamma = 1$. Time dependent averages were calculated, with the time being measured since the last equilibrium starting state. The aim was to produce the Kawasaki averages by exactly programming the dynamics in the Kawasaki distribution function (equation 7.2.19).

The phase space integral of the *bare* Kawasaki distribution function $f(t)$, equation (7.2.19), is

$$Z(t) = \int d\Gamma f(\Gamma, t) = \int d\Gamma f(\Gamma, 0) \exp\left[-\beta F_e \int_0^t ds J(-s)\right] \quad (7.7.1)$$

$Z(0)$ is the phase integral of the equilibrium distribution function which is equal to unity since $f(0)$ is the normalised equilibrium distribution function. It is interesting to consider the rate of

change of $Z(t)$ after the external field is switched on. Using manipulations based on the reversible Liouville equation we can show that,

$$\begin{aligned} \frac{d Z(t)}{dt} &= \int d\Gamma f(0) \frac{\partial}{\partial t} \exp \left[-\beta F_e \int_0^t ds J(-s) \right] \\ &= -\beta F_e \int d\Gamma f(t) J(-t) \\ &= -\beta F_e \int d\Gamma f(0) J(0) = 0 \end{aligned} \quad (7.7.2)$$

The last equality is a consequence of the Schrödinger-Heisenberg equivalence (§3.3). This implies that the bare Kawasaki distribution function is normalised for all times t . This is a direct result of the reversibility of the classical equations of motion. In Figure 7.10 we present the numerical results for $Z(t)$. Figure 7.10 shows that equation (7.7.2) is clearly false. The normalisation is unity only for a time of the order of the Lyapunov time for the system. After this time the normalisation decreases rapidly. The explanation of this apparent paradox is that the analysis used to establish (7.7.2) is based on the reversible Liouville equation. The simulation used to generate the results shown in Figure 7.10 is, however, not time reversible. Trajectories which imply a long periods (compared to the Lyapunov time) of entropy **decrease** are mechanically unstable both in nature and in computer simulations. Because it is impossible to integrate the equations of motion exactly, these entropy decreasing trajectories are not observed for times longer than the Lyapunov time which characterises the irreversible instability of the equations of motion.

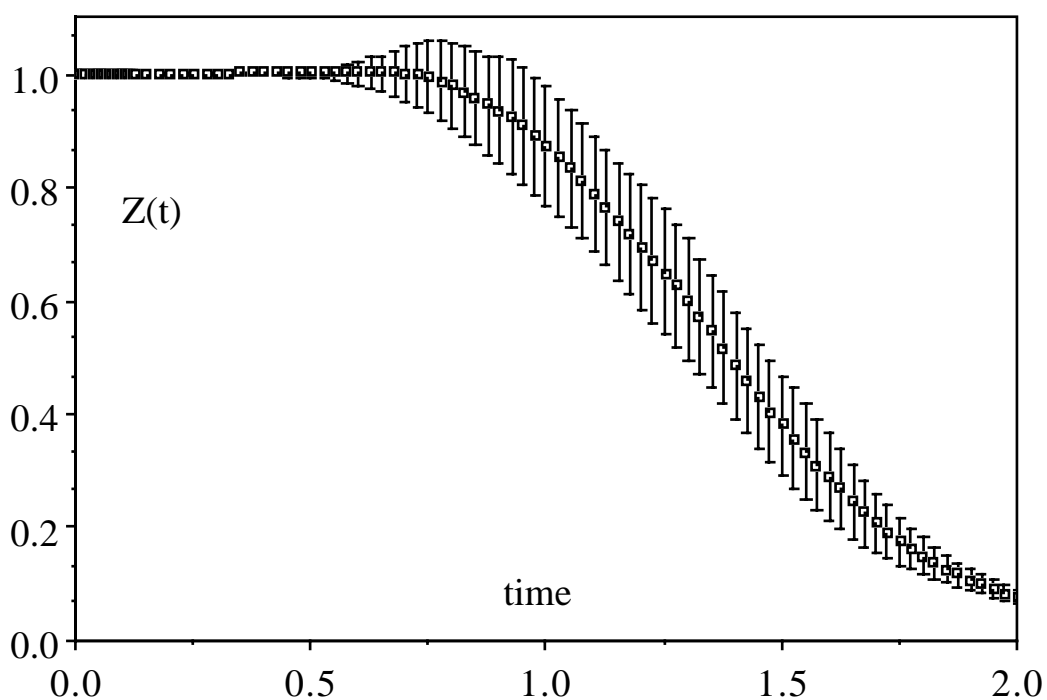


Figure 7.10

The form of the function, $Z(t)$, shown in Figure 7.10, is determined by the accuracy with which the calculations are carried out. In principle by using ever more powerful computers one could, by increasing the word length and by decreasing the integration time step, ensure that the computed $Z(t)$ stayed close to unity for longer and longer times. The exact result is that $Z(t)=1$. For a hard sphere system, the time over which the trajectory accuracy is better than a set tolerance only grows like, $-\ln(\epsilon^{1/\lambda})$ where λ is the largest Lyapunov exponent for the system and ϵ is the magnitude of the least significant digit representable on the computer. However our ability to numerically extend the times over which $Z(t)\sim 1$, is much worse than this analysis implies. As we compute (7.7.1) for longer times, the variance in $\langle \exp[-\beta F_e \int_0^t ds J(-s)] \rangle$ grows exponentially in time, regardless of the accuracy with which the trajectories are computed!

We have discussed the Kawasaki normalization in terms of numerical procedures. However exactly the same arguments apply to the experimental observation of the normalization. In nature, the problems in observing $Z(t)\sim 1$ for long times result from uncontrolled external perturbations on the system rather than from numerical errors. However numerical error can be regarded as a particular form of external perturbation (ϵ above, would then be a measure of the background noise level). Of course the act of observation itself is a source of ‘external’ noise.

The results in Figure 7.10, show that the **computed** bare Kawasaki distribution function is not be properly normalised. Thus we should not surprised to see that the bare Kawasaki expression for the average shear stress is inconsistent with the results of direct calculation as is shown in Figure 7.11.

The obvious way around this problem is to *explicitly normalise* the distribution function (Morriss and Evans, 1987). The explicitly normalised form is

$$f(t) = \frac{f(0) \exp[-\beta F_e \int_0^t ds J(-s)]}{\int d\Gamma f(0) \exp[-\beta F_e \int_0^t ds J(-s)]} \quad (7.7.3)$$

The renormalized average of the shear stress is then

$$\langle P_{xy}(t) \rangle = \frac{\int d\Gamma P_{xy}(\Gamma) f(0) \exp[-\beta F_e \int_0^t ds J(-s)]}{\int d\Gamma f(0) \exp[-\beta F_e \int_0^t ds J(-s)]} \quad (7.7.4)$$

We used computer simulation to compare the direct NEMD averages, and the bare and renormalized Kawasaki expressions for the time dependent average shear stress in a fluid. The results shown in Figure 7.11 are very encouraging. The renormalized Kawasaki result (denoted 'Kawasaki') agrees with that calculated directly and with the TTCF result. This is despite the fact that the normalisation has decreased by nearly two orders of magnitude at $t^* = 2.0$. The results show that the **bare** Kawasaki result is incorrect. It is two orders of magnitude smaller than the correct results.

Incidentally Figure 7.11 shows extraordinarily close agreement ($\sim 0.2\%$ for $0 < t^* < 2$) between the TTCF prediction and direct NEMD. The agreement between direct NEMD and TTCF results for both the hydrostatic pressure and the normal stress difference is of a similar order. This indicates that one does not need to take the thermodynamic limit for the TTCF or GK formulae to be valid. Provided correct expressions are used for the temperature and the various thermodynamic fluxes, 18 particles seems sufficient.

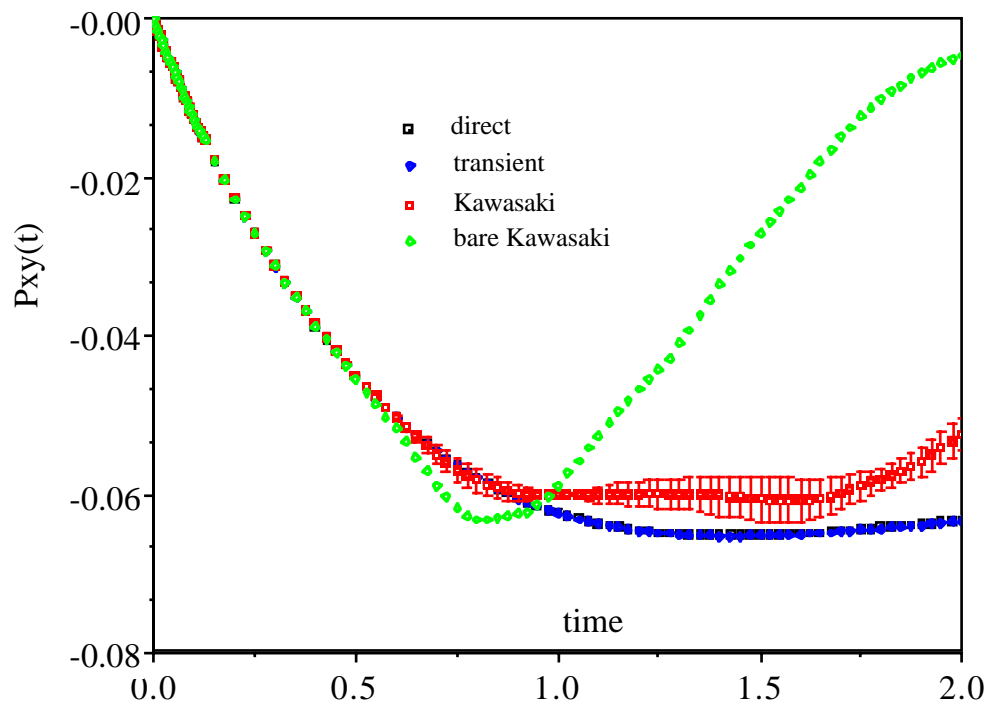


Figure 7.11

Clearly no one should plan to use the renormalized Kawasaki formalism as a routine means of computing transport coefficients. It is probably the least efficient known method for computing nonequilibrium averages. The Kawasaki formalism is however, a very important theoretical tool. It was of crucial importance to the development of nonlinear response theory and it provides an extremely useful basis for subsequent theoretical derivations. As we will see in Chapter 9, the renormalized Kawasaki formalism, in contrast to the TTCF formalism, is very

useful in providing an understanding of fluctuations in nonequilibrium steady states.

7.8 The van Kampen Objection to Linear Response theory.

Having explored some of the fundamentals of nonlinear response theory, we are now in a better position to comment on one of the early criticisms of linear response theory. In an oft-cited paper van Kampen (1971), criticised linear response theory on the basis that microscopic linearity which is assumed in linear response theory, is quite different from the macroscopic linearity manifest in linear constitutive relations. Van Kampen correctly noted that to observe linear **microscopic** response (ie of individual particle trajectories) over macroscopic time (seconds, minutes or even hours), requires external fields which are orders of magnitude smaller than those for which linear macroscopic behaviour is actually observed. Therefore, so the argument goes, the theoretical justification of, the Green-Kubo relations for linear transport coefficients, is suspect.

In order to explain his assertion that *linearity of microscopic motion is entirely different from macroscopic linearity*, van Kampen considered a system composed of electrons which move, apart from occasional collisions with impurities, freely through a conductor. An imposed external electric field, F_e , accelerates the particles between collisions. The distance an electron moves in a time t , under the influence of the field, is $1/2t^2(eF_e/m)$. In order for the induced current to be linear one requires that $t^2(eF_e/2m) \ll d$, the mean spacing of the impurities. Taking $d \sim 100\text{\AA}$ and t to be a macroscopic time, say 1 second, we see that the field must be less than $\sim 10^{-18}\text{Volts/cm!}$

As a criticism of the derivation of linear response theory, this calculation implies that for linear response theory to be valid, trajectories must be subject to a linear perturbation over macroscopic times - the time taken for experimentalists to make sensible measurements of the conductivity. This however, is incorrect.

The linear response theory expression for the conductivity, $\sigma (\equiv J/F_e)$ is,

$$\sigma = \beta V \int_0^{\infty} dt \langle J(t) J(0) \rangle_{\text{eq}} \quad (7.8.1)$$

Now it happens that in three dimensional systems the integral of the equilibrium current autocorrelation function converges rapidly. (In two dimensional systems this is expected not to be so.) The integral in fact converges in microscopic time, a few collision times in the above example. Indeed if this were not so one could never use equilibrium molecular dynamics to compute transport coefficients from the Green-Kubo formulae. Molecular dynamics is based on the assumption that transport coefficients for simple fluids can be computed from simulations which only follow the evolution systems for $\sim 10^{-10}$ seconds. These times are sufficient to ensure convergence of the Green-Kubo correlation functions for all the Navier-Stokes transport coefficients. If we require microscopic linearity over 10^{-10} seconds (rather than van Kampen's

1 second) then we see that the microscopic response will be linear for fields less than about 100Volts/cm, not an unreasonable number. It simply does not matter that for times longer than those characterising the relaxation of the relevant GK correlation function, the motion is perturbed in a nonlinear fashion. In order for linear response theory to yield correct results for linear transport coefficients, linearity is only required for times characteristic of the decay of the relevant correlation functions. These times are microscopic.

We used nonequilibrium molecular dynamics simulation of shear flow in an atomic system to explore the matter in more detail (Morriss et. al., 1989). We performed a series of simulations with and without an imposed strain rate, $\gamma (\equiv \partial u_x / \partial y)$, to measure the actual separation d , of phase space trajectories as a function of the imposed strain rate. The phase space separation is defined to be,

$$d(t, \gamma) \equiv \sqrt{(\mathbf{\Gamma}(t, \gamma) - \mathbf{\Gamma}(t, 0))^2} \quad (7.8.2)$$

where $\mathbf{\Gamma} \equiv (\mathbf{q}_1, \mathbf{q}_2, \dots, \mathbf{q}_N, \mathbf{p}_1, \mathbf{p}_2, \dots, \mathbf{p}_N)$ is the $6N$ -dimensional phase space position for the system. In measuring the separation of phase space trajectories we imposed the initial condition that at time zero the equilibrium and nonequilibrium trajectories start from **exactly** the same point in phase space, $d(0, \gamma) = 0, \forall \gamma$. We used the 'infinite checker board' convention for defining the Cartesian coordinates of a particle in a periodic system. This eliminates trivial discontinuities in these coordinates. We also reported the ensemble average of the phase space separation, averaged over an equilibrium ensemble of initial phases, $\mathbf{\Gamma}(0, 0)$.

The equations of motion employed were the SLLOD equations. As we have seen the linear response computed from these equations is given precisely, by the Green-Kubo expression for the shear viscosity. The system studied in these simulations was the Lennard-Jones fluid at its triple point ($\rho^* = \rho \sigma^3 = 0.8442, T^* = k_B T / \epsilon = 0.722, t^* = t(\epsilon/m)^{1/2} \sigma^{-1}$). A Lees-Edwards periodic system of 256 particles with a potential truncated at, $r^* = r/\sigma = 2.5$, was employed.

Before we begin to analyse the phase separation data we need to review some of the relevant features of Lennard-Jones triple point rheology. Firstly, as we have seen (§6.3) this fluid is shear thinning. The strain rate dependent shear viscosities of the Lennard-Jones triple point fluid are set out in the table below.

Table 7.3
Strain rate dependent shear viscosities for the Triple Point Lennard-Jones fluid

reduced strain rate	reduced viscosity		percentage nonlinearity
1.0	2.17	± 0.03	37%
0.1	3.04	± 0.03	12%
0.01	3.31	± 0.08	~4%
0.0	3.44	± 0.2	0% NEMD est

The most important relevant fact that should be noted from these results is that for reduced strain rates, $\dot{\gamma}^* < \sim 10^{-2}$, the fluid is effectively Newtonian with a viscosity which varies at most, by less than ~4% of its zero shear value. (Because of the uncertainty surrounding the zero shear viscosity, we cannot be more certain about the degree of nonlinearity present at $\dot{\gamma}^* = 0.01$.)

The second relevant fact that we should remember is that the GK equilibrium time correlation function whose integral gives the shear viscosity, has decayed to less than 1% of its zero time value at a reduced time $t^* = 2.0$. Values are shown below.

Table 7.4
Green Kubo equilibrium stress correlation function for shear viscosity

t^*	correlation function	percentage of $t=0$ value
0.0	24.00	100%
0.1	7.17	29%
1.0	0.26	1%
2.0	0.09	0.3%

Of course the viscosity which is the time integral of this correlation function converges relatively slowly due to the presence of the slowly decaying $t^{-3/2}$ long time tail. Here again there

is some uncertainty. If one believes that *enhanced long time tail* phenomena (§6.3), are truly asymptotic and persist indefinitely then one finds that the viscosity converges to within $\sim 13\%$ of its asymptotic value at $t^*=1.0$ and to within $\sim 5\%$ of the asymptotic value at $t^*=10.0$. (If we map our simulation onto the standard Lennard-Jones representation of argon, $t^*=1.0$ corresponds to a time of 21.6 picoseconds.) If *enhanced long time tails* are not asymptotic then the GK integrand for the shear viscosity converges to within $\sim 5\%$ of its infinite time value by $t^*=2$.

The only important observation that concerns us here is that the GK estimate for the shear viscosity is determined in **microscopic** time, a few hundreds of picoseconds at the very most, for argon. This observation was omitted from van Kampen's argument. We call the range of times required to ensure say 5%, convergence of the GK expression for the viscosity, the *GK time window*.

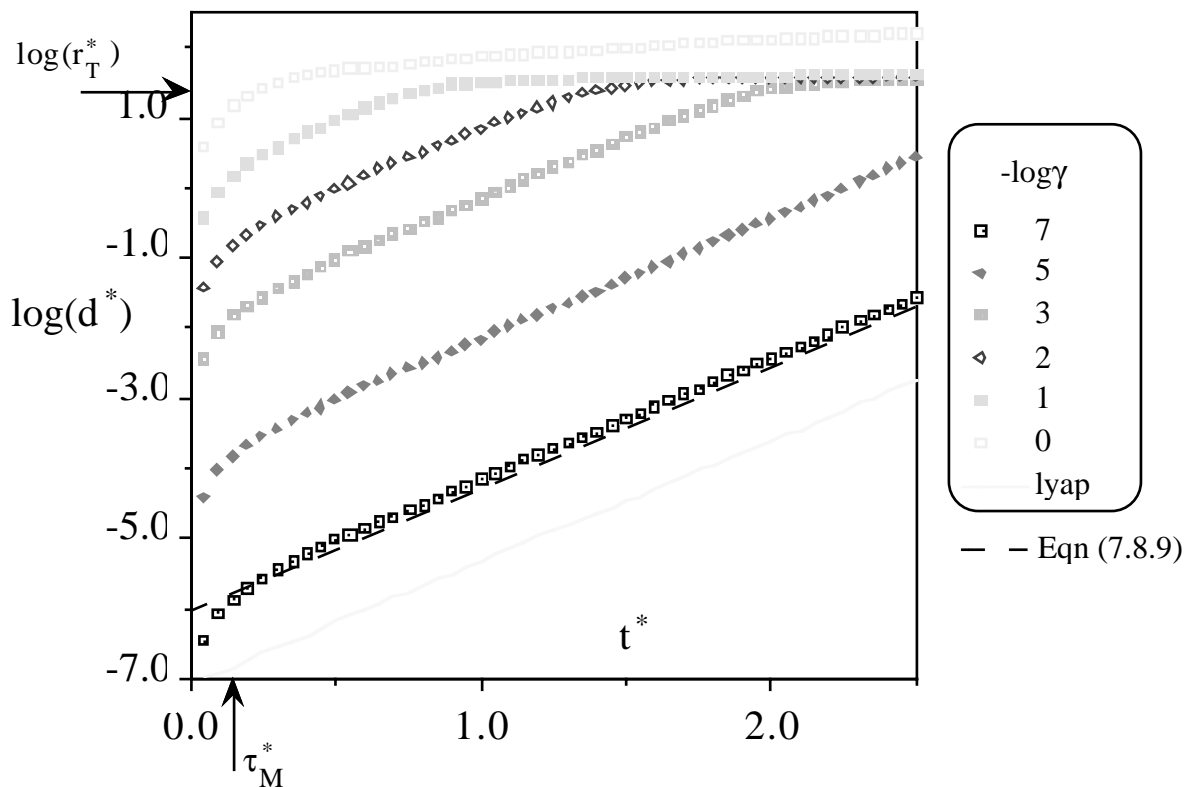


Figure 7.12

Figure 7.12 shows the common logarithm of the ensemble average of the phase space separation plotted as a function of reduced time for various values of the imposed shear rate. The shear rates employed were: $\gamma^*=1.0, 10^{-1}, 10^{-2}, 10^{-3}, 10^{-5}, 10^{-7}$. Note that for the standard Lennard-Jones argon representation, these strain rates correspond to shear rates of $4.6 \cdot 10^{11}$ to $4.6 \cdot 10^5$ Hz. It will be clear from the present results that no new phenomena would be revealed at strain rates less than $\gamma^* \sim 10^{-4}$.

One can see from the figure that at a shear rate of 10^{-7} , the phase space separation increases very rapidly initially and then slows to an exponential increase with time. The same pattern is followed at a strain rate of 10^{-5} except that the initial rise is even more rapid than for a

strain rate of 10^{-7} . Remember that at $t=0$ the phase space separations start from zero, and therefore the logarithm of the $t=0$ separations is $-\infty$, for all strain rates.

For strain rates $>10^{-5}$, we notice that at long times the phase separation is a constant independent of time. We see an extremely rapid initial rise, followed by an exponential increase with a slope **which is independent of strain rate**, followed at later times by a plateau. The plateau is easily understood.

The simulations shown in Figures 7.12,13 are carried out at constant peculiar kinetic energy $\Sigma p_i^2/2m = 3Nk_B T$. The $3N$ components of the phase space momenta therefore lie on the surface of a $3N$ -dimensional sphere of radius, $r_T = \sqrt{(3Nmk_B T)}$. Once the phase space separation exceeds this radius, the curved nature of accessible momentum space will be apparent in our phase space separation plots. The arrow marked on Figure 7.12 shows when the logarithm of the separation is equal to this radius. The maximum separation of phase points within the momentum sub-space is of course $2r$. It is clear therefore that the exponential separation must end at approximately, $d(t,\Gamma) = r_T$. This is exactly what is observed in Figure 7.12.

Between the plateau and the initial (almost vertical) rise is an exponential region. As can be seen from the graph the slope of this rise is virtually independent of strain rate. The slope is related to the largest positive Lyapunov exponent for the system at equilibrium. The Lyapunov exponent measures the rate of separation of phase trajectories that start a small distance apart, but which are governed by identical dynamics. After initially being separated by the external field, the rate of phase space separation thereafter is governed by the usual Lyapunov instability. The fact that the two trajectories employ slightly different dynamics is a second order consideration. The Lyapunov exponents are known to be insensitive to the magnitude of the perturbing external field for field strengths less than 10^{-2} .

This conjecture regarding the role played by the Lyapunov exponent in the separation of equilibrium and nonequilibrium trajectories which start from a common phase origin is easily verified numerically. Instead of measuring the separation, d , induced by the strain rate, we ran a simulation in which two trajectories started at slightly different phases and which evolved under (identical) zero strain rate equations of motion. The resulting displacement is shown in Figure 7.12 and labelled as 'lyap' in the legend. One can see that the slope of this Lyapunov curve is essentially identical to the exponential portions of the strain rate driven curves. The time constants for the exponential portions of the curves are given in Table 7.5.

At this stage we see that even at our smallest strain rate, the trajectory separation is exponential in time. It may be thought that this exponential separation in time supports van Kampen's objection to linear response theory. Surely exponentially diverging trajectories imply nonlinearity? The assertion turns out to be false.

Table 7.5
Exponential time Constants for phase separation in the Triple Point Lennard-Jones fluid under shear

time constant	reduced strain rate	
1.715 ± 0.002	0.0	Lyapunov
1.730 ± 0.002	10 ⁻⁷	shear induced
1.717 ± 0.002	10 ⁻⁵	"
1.708 ± 0.012	10 ⁻³	"
1.689 ± 0.03	10 ⁻²	"

In Figure 7.13 we examine the field dependence of the phase separations in more detail. In this figure we plot the ratio of the separations to the separation observed for a field, $\gamma^* = 10^{-7}$.

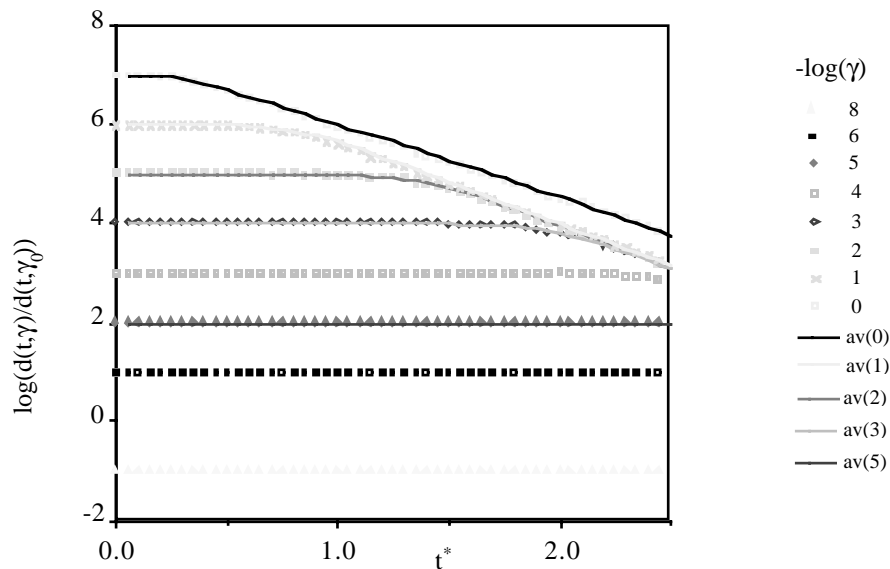


Figure 7.13

If the ensemble averaged trajectory response is linear then each of the curves in Figure 7.13 will be equispaced horizontal lines. The curves denoted 'av' refer to the ensemble averaged separations shown in Figure 7.12. One can see immediately that within the GK time window, $t^* < 2.0$, all the separations are linear in the field except for the largest two strain rates $\gamma^* = 1.0, 0.1$. We should expect that all strain rates exhibiting linearity within the GK time window should correspond to those systems exhibiting macroscopic linear behaviour (ie. those which are Newtonian). Those exhibiting microscopic nonlinearity within the GK time window should display non-Newtonian macroscopic behaviour. Comparing table 7.3 with Figure 7.12, this is

exactly what is seen.

Although systems at a shear rate $\gamma^*=10^{-2}$ & 10^{-4} , do exhibit a nonlinear growth in the phase space separation, it occurs at times which are so late, that it cannot possibly effect the numerical values of the shear viscosity. These nonlinearities occur outside the GK time window.

A possible objection to these conclusions might be: since we are computing ensemble **averages** of the phase space separations, it might be the averaging process which ensures the observed microscopic linearity. Individual trajectories might still be perturbed nonlinearly with respect to the strain rate. This however, is not the case. In Figure 7.13 the symbols plotted represent the phase space separation induced in **single** trajectories. For all strain rates a common phase origin is used. We did not average over the time zero phase origins of the systems.

What we see is a slightly noisier version of the ensemble averaged results. Detailed analysis of the un-averaged results reveals that:

1. for $\gamma^* < 10^{-2}$ linearity in strain rate is observed for individual trajectories; and
2. the exponential behaviour in time is only observed when $d(\gamma,t)$ is averaged over some finite but small, time interval.

The exponential Lyapunov separation is of course only expected to be observed 'on average' either by employing time or ensemble averages. The main point we make here is that even for individual trajectories where phase separation is not exactly exponential in time, trajectory separation is to 4 significant figure accuracy, linear in the field. The linearity of the response is not produced by ensemble averaging.

We conclude from these studies that within the GK time window, macroscopic and microscopic linearity are observed for identical ranges of strain rates. For times shorter than those required for convergence of the linear response theory expressions for transport coefficients, the individual phase space trajectories are perturbed linearly with respect to the strain rate for those values of the strain rate for which the fluid exhibits linear macroscopic behaviour. This is in spite of the fact that within this domain the strain rate induces an exponential separation of trajectories with respect to time. We believe that many people have assumed an exponential trajectory separation in time implies an exponential separation with respect to the magnitude of the external field. This work shows that within the GK time window, the dominant microscopic behaviour in fluids which exhibit linear macroscopic behaviour, is linear in the external field but exponential in time.

We have seen in Figure 7.12 that for intermediate times the phase separation takes the form,

$$d = A\gamma \exp[t/\tau_L] \quad (7.8.5)$$

where the *Lyapunov time*, τ_L , is the inverse of the largest Lyapunov exponent for the system at equilibrium. We can explain why the phase separation exhibits this functional form and moreover, we can make a rough calculation of the absolute magnitude of the coefficient, A. We know that the exponential separation of trajectories only begins after a time which is roughly the Maxwell relaxation time τ_M , for the fluid. Before the particles sense their mutual interactions, the particles are freely streaming with trajectories determined by the initial values of $(d\mathbf{q}/dt, d\mathbf{p}/dt)$. After this initial motion the particles will have coordinates and momenta as follows,

$$\begin{aligned} \mathbf{q}_i(t) &= \mathbf{q}_i(0) + \left[\frac{\mathbf{p}_i(0)}{m} + \mathbf{i}\gamma y_i(0) \right] t \\ \mathbf{p}_i(t) &= \mathbf{p}_i(0) + [\mathbf{F}_i(0) - \mathbf{i}\gamma \mathbf{p}_{yi}(0)] t \end{aligned} \quad (7.8.6)$$

When this approximation breaks down, approximately at the Maxwell relaxation time, $\tau_M \equiv \eta/G$, the phase separation $d(\tau_M, \gamma)$ will be,

$$d(\tau_M, \gamma) = \gamma \tau_M \sqrt{\sum_{i=1}^N [y_i^2(0) + p_{yi}^2(0)]} \quad (7.8.7)$$

For our system this distance is,

$$d(\tau_M, \gamma) = \gamma \tau_M \left\{ \frac{N^{5/3}}{3n^{2/3}} + NT \right\}^{1/2} \sim 8.7\gamma \quad (7.8.8)$$

We have used the fact that the reduced Maxwell time is 0.137. After this time the phase separation can be expected to grow as,

$$d(\gamma, t) \sim d(\gamma, \tau_M) \exp\left[\frac{t}{\tau_L + O(\gamma^2)} \right] \quad (7.8.9)$$

where, as before τ_L is the inverse of the largest zero-strain rate Lyapunov exponent. For fields less than $\gamma^* = 10^{-2}$, the equilibrium Lyapunov time dominates the denominator of the above expression. This explains why the slopes of the curves in Figure 7.12 are independent of strain rate. Furthermore by combining equations (7.8.5, 8.9) we see that in the regime where the strain rate corrections to the Lyapunov exponents are small, the phase separation takes the form given by equation (7.8.5) with the coefficient, $A \sim 8.7$. Equation (7.8.9) is plotted, for a reduced strain rate of 10^{-7} , as a dashed line in Figure 7.12. It is in reasonable agreement with the results. The results for other strain rates are similar. The greatest uncertainty in the prediction is the

estimation of the precise time at which Lyapunov behaviour begins.